JCB Journal of Cell Biology

ARTICLE

Differential requirement for Bub1 and Bub3 in regulation of meiotic versus mitotic chromosome segregation

Gisela Cairo, Anne M. MacKenzie, and Soni Lacefield

Accurate chromosome segregation depends on the proper attachment of kinetochores to spindle microtubules before anaphase onset. The Ipl1/Aurora B kinase corrects improper attachments by phosphorylating kinetochore components and so releasing aberrant kinetochore–microtubule interactions. The localization of Ipl1 to kinetochores in budding yeast depends upon multiple pathways, including the Bub1–Bub3 pathway. We show here that in meiosis, Bub3 is crucial for correction of attachment errors. Depletion of Bub3 results in reduced levels of kinetochore-localized Ipl1 and concomitant massive chromosome missegregation caused by incorrect chromosome–spindle attachments. Depletion of Bub3 also results in shorter metaphase I and metaphase II due to premature localization of protein phosphatase 1 (PP1) to kinetochores, which antagonizes Ipl1-mediated phosphorylation. We propose a new role for the Bub1–Bub3 pathway in maintaining the balance between kinetochore localization of Ipl1 and PP1, a balance that is essential for accurate meiotic chromosome segregation and timely anaphase onset.

Introduction

Faithful chromosome segregation in meiosis relies on proper attachment of chromosomes to spindle microtubules. These attachments form through kinetochores, large protein complexes assembled on centromeres that bind microtubules. In meiosis, DNA replication is followed by two rounds of chromosome segregation for the formation of haploid gametes from a diploid progenitor. In meiosis I, the kinetochores on the two sister chromatids are linked together and assemble one microtubule-binding site (Marston and Wassmann, 2017). The coorientation of sister kinetochores allows the kinetochores of the paired homologous chromosomes to attach to microtubules emanating from opposite spindle poles for segregation in anaphase I. In meiosis II, sister kinetochores no longer coorient but instead attach to opposite spindle poles for segregation in anaphase II.

The cell has developed mechanisms for correcting errors in kinetochore–microtubule attachments. For example, if kinetochores of homologous chromosomes are attached to microtubules emanating from the same spindle pole in meiosis I, Ipl1/Aurora B kinase phosphorylates kinetochore proteins to drive release of the attachments (Monje-Casas et al., 2007; Saurin, 2018; Yu and Koshland, 2007). This error-correction mechanism gives the kinetochore another opportunity to make proper attachments. In mitosis and presumably in meiosis, there is a balance between Ipl1/Aurora B kinase activity and protein phosphatase 1 (PP1) activity. Once proper kinetochore–microtubule attachments are made, PP1 binds to the kinetochore and counteracts Ipl1/Aurora B by dephosphorylating Aurora B/Ipl1 substrates, stabilizing microtubule–kinetochore attachments (Liu et al., 2010; Meadows et al., 2011; Nijenhuis et al., 2014; Rosenberg et al., 2011; Suzuki et al., 2018).

In both mitosis and meiosis, the spindle checkpoint monitors kinetochore–microtubule attachments and will send a signal to delay anaphase onset if kinetochores are unattached. To initiate spindle checkpoint signaling, either protein kinase Mps1 or Polo phosphorylates kinetochore protein Knl1/Spc105 on MELT motifs (Espeut et al., 2015; London et al., 2012; Primorac et al., 2013; Shepperd et al., 2012; Yamagishi et al., 2012). Spindle checkpoint protein Bub3 binds to the phosphorylated MELT motifs and also binds Bub1. Bub1 can recruit other spindle checkpoint proteins, ultimately resulting in the formation of the mitotic checkpoint complex that inhibits the activity of the anaphase-promoting complex/cyclosome (APC/C) to delay anaphase onset until correct attachments are made (Saurin, 2018).

In addition to their role in spindle checkpoint signaling, two spindle checkpoint proteins, Bub1 and Bub3, also ensure that

Department of Biology, Indiana University, Bloomington, IN.

Correspondence to Soni Lacefield: sonil@indiana.edu.

chromosomes biorient, or attach to opposite spindle poles. For its role in biorientation in meiosis and mitosis, Bub1 phosphorylates histone H2A, which recruits shugoshin (Indjeian et al., 2005; Kawashima et al., 2010; Kiburz et al., 2008; Marston and Wassmann, 2017). Budding yeast and *Drosophila melanogaster* have a single shugoshin (Sgo1 and mei-S332, respectively), whereas fission yeast and mammals have two shugoshins (Sgo1 and Sgo2; Katis et al., 2010; Kerrebrock et al., 1992; Kitajima et al., 2004; Kitajima et al., 2006; Marston et al., 2004; Rabitsch et al., 2004; Salic et al., 2004). Shugoshins are also required for the protection of centromeric cohesion in meiosis I. Shugoshins function by serving as a platform for the binding of effector proteins such as PP2A, condensin, and the chromosome passenger complex (CPC), of which Ipl1/Aurora B is a subunit (Marston, 2015). Evidence suggests that recruitment of condensin helps biorient chromosomes by biasing kinetochore capture (Peplowska et al., 2014; Verzijlbergen et al., 2014).

In mitosis, several other pathways can recruit Ip11/Aurora B to the kinetochore, in addition to the Bub3–Bub1 pathway. For example, the CPC binds histone H3 when phosphorylated by haspin kinases (Edgerton et al., 2016; Kelly et al., 2010; Niedzialkowska et al., 2012; Wang et al., 2010; Yamagishi et al., 2010). In budding yeast, two additional pathways are also known to recruit Ipl1 (the budding yeast Aurora B homologue): (1) the CPC binds to kinetochore protein Ndc10, a subunit of the Cbf3 centromere-binding complex, and (2) Sli15-Ipl1 binds to the inner kinetochore COMA complex, composed of Ctf19, Okp1, Mcm21, and Ame1 (Cho and Harrison, 2011; Fischböck-Halwachs et al., 2019; Garcia-Rodriguez et al., 2019; Yoon and Carbon, 1999). In budding yeast mitosis, loss of any one of these pathways does not severely disrupt chromosome biorientation but may cause an increase in aneuploidy. However, loss of Ipl1 kinase severely disrupts chromosome biorientation, such that most chromosomes are pulled to one spindle pole (Tanaka et al., 2002). These findings suggest that the multiple recruitment pathways are somewhat redundant in ensuring that Ipl1 is kinetochore localized for error correction of aberrant kinetochore–microtubule attachments in mitosis. Whether the recruitment pathways also have redundant roles in meiosis has not been tested.

Here, we test the importance of Ipl1 recruitment through Bub1 and Bub3 in meiosis. We find that the loss of Bub1, Bub3, or Sgo1 causes a shorter metaphase I and II and massive chromosome missegregation, especially in meiosis II. In sharp contrast, loss of *BUB1* and *BUB3* in mitosis causes a longer metaphase and does not cause massive chromosome missegregation (Kim et al., 2017; Kim et al., 2015; Warren et al., 2002; Yang et al., 2015). We show that the meiotic phenotypes of increased chromosome missegregation and the shorter duration of metaphase I and II are due to lower levels of Ipl1 at the kinetochore. Because Ipl1 and PP1 counteract one another, we asked whether the shorter duration to anaphase onset was due to premature PP1 at the kinetochore. Our results demonstrate that attenuation of kinetochore binding of PP1 suppressed the short metaphase phenotype of Bub1- or Bub3-depleted cells. Overall, our results demonstrate that the Ipl1 kinetochore recruitment pathway through Bub1, Bub3, and Sgo1 is essential for meiosis. In addition, we show that the balance between kinetochore-localized Ipl1 and PP1 sets the duration of meiosis.

Results

Anaphase I and II onset occurs prematurely in cells depleted of Bub1, Bub3, and Sgo1

To investigate the role of Bub3 in meiotic progression, we used the anchor-away technique to deplete Bub3 from the nucleus at meiotic entry (Haruki et al., 2008). We chose to use anchor away instead of deleting *BUB3* because homozygous *bub3Δ* cells can become aneuploid (Warren et al., 2002). By depleting Bub3 from the nucleus just before meiotic initiation, we avoid any mitotic defects that arise from loss of Bub3. The cells expressed *BUB3* tagged with FRB (FKBP12-rapamycin–binding domain), and the ribosomal protein Rpl13a was tagged with FKBP12. Upon addition of rapamycin, FRB and FKBP12 make a stable interaction, leading to the removal of Bub3 from the nucleus, ∼30 min after rapamycin addition (Fig. S1, A and B). Two assays verified that the tag did not disrupt Bub3 function in the absence of rapamycin but did give a phenotype similar to *bub3Δ* cells in the presence of rapamycin. First, cells expressing Bub3-FRB were only mildly sensitive to the microtubule-depolymerizing drug benomyl. In contrast, with addition of rapamycin, cells did not grow on benomyl, suggesting that they lost mitotic spindle checkpoint activity (Fig. S1 C). Second, we find that Bub3-FRB cells sporulated normally, but when rapamycin was added they produced only inviable spores, suggesting that Bub3 was depleted from the nucleus in meiosis (Fig. S2, A and B). These results are consistent with Bub3-FRB depletion from the nucleus if rapamycin is present. Similarly, because Bub3 forms a complex with Bub1 at the kinetochore, we also tested the nuclear depletion of Bub1 using the anchor-away technique, which displayed similar results as the nuclear depletion of Bub3 (Figs. S1 C and S2, A and B).

To monitor the duration of each meiotic stage, cells expressed Spc42, a spindle pole body (SPB) component, tagged with mCherry; Zip1, a synaptonemal complex component tagged with GFP; and Tub1, α-tubulin that incorporates into microtubules, tagged with GFP (Bullitt et al., 1997; Scherthan et al., 2007; Sym et al., 1993). Although both Zip1 and Tub1 are tagged with GFP, the proteins are temporally and morphologically distinguishable (Tsuchiya et al., 2011; Tsuchiya et al., 2014). The synaptonemal complex assembles and disassembles in prophase I, showing a nuclear haze of Zip1-GFP that disappears before SPB separation and spindle assembly (Carminati and Stearns, 1997; Scherthan et al., 2007; Sym et al., 1993; Fig. 1 A). We used time-lapse microscopy, taking images every 10 min throughout meiosis. To assess metaphase duration, we measured the time from SPB separation to the initiation of anaphase I spindle elongation and the time from SPB separation in meiosis II to the initiation of anaphase II spindle elongation.

With the nuclear depletion of Bub3 and Bub1 before meiotic initiation, the onset of both anaphase I and anaphase II were shorter in duration than in the wild-type control cells (Fig. 1, B and C). Anaphase I onset was ∼14 min shorter and anaphase II onset was ∼23 min shorter in Bub3-depleted cells than in

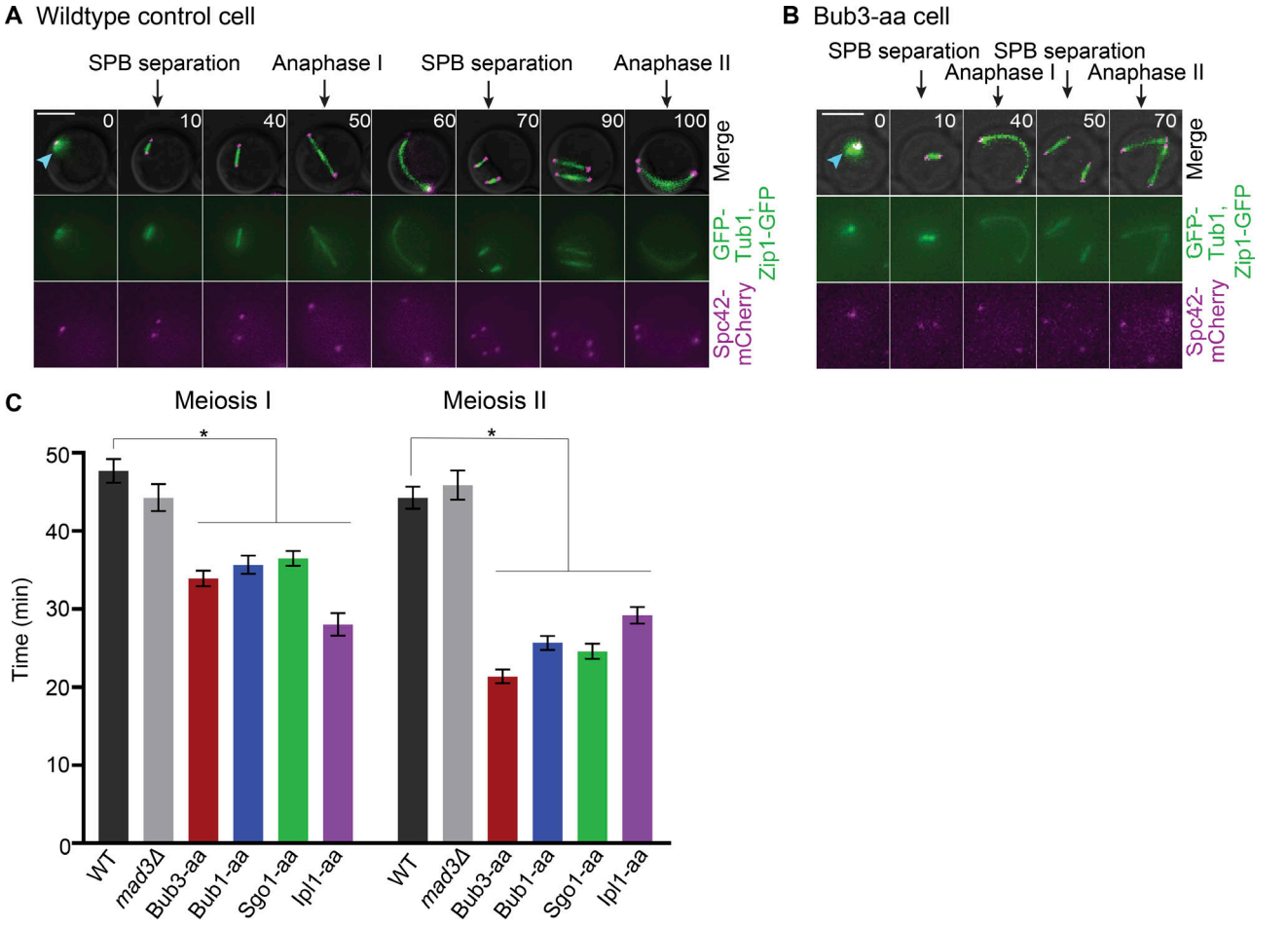

Figure 1. **Bub3, Bub1, Sgo1, and Ipl1 prevent premature anaphase I and II onset. (A and B)** Representative time-lapse images of a wild-type anchor-away control cell (A) and a cell with Bub3 nuclear depletion (Bub3-aa, anchor away; B). Rapamycin was added at meiotic entry. Cells express Spc42-mCherry, GFP-Tub1, and Zip1-GFP. Arrowheads mark Zip1-GFP nuclear localization. Time 0 marks prophase I. Scale bars, 5 µm. **(C)** Graph of the mean time from SPB separation in meiosis I to anaphase I onset and SPB separation in meiosis II to anaphase II onset. At least 100 cells from two or more independent experiments per genotype were monitored with rapamycin addition. Asterisks indicate a statistically significant difference compared with wild-type anchor-away control cells (*, $P < 0.05$, Mann-Whitney test). Error bars represent SEM. aa, anchor away.

wild-type cells. These results were unexpected because we and others showed that loss of *BUB3* or *BUB1* in mitosis delays mitotic anaphase onset (Kim et al., 2015; Yang et al., 2015). Therefore, our results suggest that the roles of Bub3 and Bub1 in regulating anaphase onset are different in meiosis than in mitosis.

Although spindle elongation is often used as a marker of anaphase onset, some genetic perturbations can cause premature spindle elongation before a true transition into anaphase I or II (Shonn et al., 2000). Therefore, we verified whether spindle elongation appropriately coincided with anaphase onset in Bub3-depleted cells by monitoring another marker for anaphase, the release of the Cdc14 phosphatase from the nucleolus. Cdc14 is normally sequestered in the nucleolus until anaphase I, when it is released; after anaphase I onset, it is resequestered and then released again in anaphase II (Marston et al., 2003). We tagged Cdc14 with GFP in cells expressing Spc42-mCherry. In meiosis I, all Bub3-depleted cells released Cdc14-GFP from the nucleolus upon anaphase I spindle elongation, similar to wild-type cells (Fig. S3, A–C). In meiosis II, 92% of Bub3-depleted cells released Cdc14 upon spindle elongation. Therefore, in most cells, anaphase spindle elongation coincides with anaphase onset in Bub3-depleted cells. We conclude that Bub3 is crucial for the normal timing of anaphase onset.

In addition to the activation of spindle checkpoint signaling, the kinetochore-localized Bub3–Bub1 complex is also required for the recruitment of Sgo1 to the kinetochore (Marston, 2015). That localization is important for centromeric cohesion in meiosis I and promotes chromosome biorientation. We asked which role of Bub1, spindle checkpoint signaling or Sgo1 recruitment, was important for the normal duration of meiosis. Deletion of *MAD3*, which encodes a spindle checkpoint protein that incorporates into the mitotic checkpoint complex for checkpoint signaling, did not result in premature anaphase I or II onset (Fig. 1 C). In contrast, nuclear depletion of Sgo1 through anchor away resulted in a shorter duration to anaphase I and II onset compared with the wild-type control strain (Fig. 1 C). These results suggest that the role of Bub1 in recruiting Sgo1 to the kinetochore is important for setting the normal duration of meiosis.

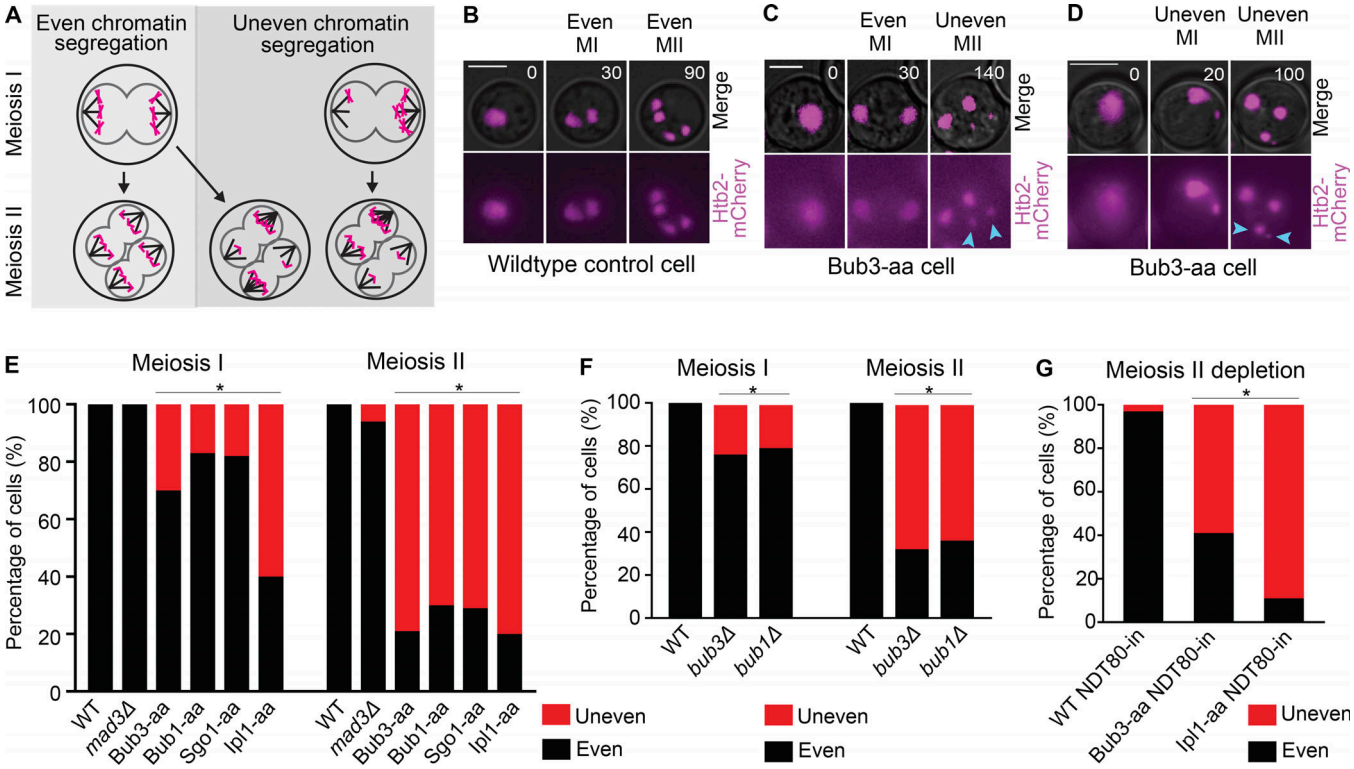

Figure 2. **Cells with nuclear depletion of Bub3 display massive chromatin missegregation in meiosis. (A)** Schematic of even and uneven chromatin segregation in meiosis I and II. **(B–D)** Representative time-lapses of wild-type cells (B) and cells with nuclear depletion of Bub3 (Bub3-aa) displaying even (C) and uneven (D) chromatin segregation in meiosis I and uneven segregation in meiosis II. Cells express Htb2-mCherry to visualize chromatin. Time 0 marks metaphase I. Scale bars, 5 µm. **(E and F)** Percentage of cells that display even and uneven chromatin segregation in meiosis I and meiosis II, with either anchor-away (E) or deletion (F) strains. Asterisks indicate a statistically significant difference compared with the wild-type cells (*, $P < 0.05$, two-tailed Fisher's exact test). 100 cells (E) and 75 cells (F) from two or more independent experiments per genotype were monitored. **(G)** Percentage of cells that display even and uneven chromatin segregation with nuclear depletion of Bub3 or Ipl1 in meiosis II only using Ndt80-in to synchronize cells and then adding rapamycin when cells were completing meiosis I. Asterisks indicate a statistically significant difference compared with the wild-type cells (*, $P < 0.05$, two-tailed Fisher's exact test). 100 cells from two or more independent experiments per genotype were monitored. aa, anchor away.

Cells depleted of Bub3 and Bub1 undergo massive chromosome missegregation in meiosis

We noticed that the spores that formed after meiosis in Bub3- and Bub1-depleted cells often varied in sizes within the same ascus in strong contrast to the production of four spores of equivalent sizes in wild-type cells (data not shown). Because spores are packaged mainly around the nucleus, we speculated that the amount of chromatin was different in each spore due to massive chromosome missegregation, creating some spores with more chromatin than other spores (Neiman, 2011). To monitor the segregation of chromatin, we tagged histone Htb2 with mCherry and performed time-lapse microscopy. We then quantified the areas of the two fluorescent masses after the first meiotic division and the four masses after the second meiotic divisions in wild-type cells and cells depleted of nuclear Bub3, Bub1, or Sgo1 (Fig. 2, A–D). We found that after meiosis I, 30% of Bub3-depleted cells and 17% of Bub1-depleted cells have uneven chromatin segregation, where uneven means greater than one SD from wild type (Fig. 2 E). The defect is more penetrant in meiosis II; 79% of Bub3-depleted cells and 70% of Bub1-depleted cells have uneven chromatin segregation (Fig. 2 E). Similar to Bub1 depletion, Sgo1 depletion leads to 18% and 71% uneven chromatin segregation in meiosis I and II, respectively (Fig. 2 E). Although the meiosis II defect is cumulative, in that it represents both the meiosis I and II defects, the data still suggest that meiosis II has a much more penetrant defect than meiosis I.

We were surprised that the defect in chromatin segregation was stronger in meiosis II than in meiosis I and questioned whether this could be due to increased nuclear depletion of Bub3 or Bub1 as meiosis progresses. To address this question, we measured the size of chromatin masses in cells with a complete deletion of *BUB3* or *BUB1*. We found that, similar to our anchor-away strains, there is an enhanced phenotype in meiosis II. The *bub3Δ* cells display 24% and 68% uneven chromatin segregation in meiosis I and II, respectively (Fig. 2 F). The *bub1Δ* cells display 20% and 64% uneven chromatin segregation in meiosis I and II, respectively. Because deletion strains display similar phenotypes to the strains in which Bub3 or Bub1 was anchored away, we conclude that the more penetrant phenotype in meiosis II is not due to differences in the amount of Bub1 or Bub3 depleted from the nucleus.

The meiosis II phenotype described above could be an indirect consequence of the loss of Bub3 earlier in meiosis or it could be due to the loss of Bub3 in meiosis II. To distinguish between these possibilities, we depleted Bub3 at the end of meiosis I. We synchronized strains by using the inducible Ndt80 (*NDT80-in*)

system, in which the middle meiosis transcription factor is placed under the control of the inducible *GAL1,10* promoter, and cells express GAL4 fused to the estrogen receptor (Benjamin et al., 2003; Carlile and Amon, 2008). Cells arrest at prophase I in the absence of Ndt80, and then the addition of β-estradiol induces the expression of *NDT80*, releasing the cells from a prophase I arrest. We added rapamycin 3 h after the addition of β-estradiol and scored cells that underwent anaphase II ∼40 min after rapamycin addition, as these cells would then enter meiosis II without Bub3. We found that 59% of cells displayed massive chromatin missegregation (Fig. 2 G). These results suggest that the chromatin missegregation defect is a consequence of the loss of Bub3 in meiosis II and not an indirect consequence of a defect earlier in meiosis.

The high penetrance of uneven chromatin segregation in cells with Bub3 nuclear depletion was specific to meiosis. Only 2% of cells showed uneven chromatin segregation in mitosis (Fig. 3, A–D). Although cells that lack Bub3 have a higher chromosome missegregation frequency than wild-type cells in mitosis (Warren et al., 2002), the aneuploidy of a single chromosome is likely not detected with this assay. We therefore measured the percent missegregation of a single chromosome in mitosis by tagging chromosome IV with an array of Lac operators (LacOs) in a strain that expresses GFP fused to the Lac repressor (GFP-LacI). Using time-lapse microscopy, we monitored the segregation of the GFP focus and found that cells with depletion of Bub3 displayed chromosome missegregation in 1.5% of mitotic divisions (Fig. 3, E–G). These results suggest that Bub3 has a more important role in meiotic chromosome segregation than mitotic chromosome segregation.

Ipl1 levels at the kinetochore are low in Bub3-, Bub1-, and Sgo1-depleted cells

The uneven chromatin segregation phenotype was reminiscent to that seen in mitosis when cells with a temperature-sensitive mutation of the Aurora B kinase homologue Ipl1 were grown at the restrictive temperature or in meiosis when Ipl1 was not expressed (Meyer et al., 2013; Monje-Casas et al., 2007; Tanaka et al., 2002; Yu and Koshland, 2007). Ipl1 corrects improper kinetochore–microtubule attachments by phosphorylating kinetochore proteins to release attachments that are not under tension (London and Biggins, 2014). In both mitosis and meiosis, initial chromosome attachments are biased to the old SPB, and Ipl1 is required to release improper attachments for error correction (Meyer et al., 2013; Tanaka et al., 2002). In the absence of Ipl1, chromosomes cannot correct initial attachments, and, subsequently, most chromosomes stay attached to the old SPB.

We used anchor away to deplete Ipl1 from the nucleus in cells expressing Htb2-mCherry. We measured chromatin mass size and found that loss of Ipl1 caused an uneven chromatin segregation phenotype in mitosis, meiosis I, and meiosis II (Figs. 2, E and G; and 3, A–D). In mitosis, 82% of cells with nuclear depletion of Ipl1 displayed an uneven chromatin segregation phenotype (Fig. 3 D). Monitoring mitotic chromosome IV segregation showed that 76% of divisions resulted in chromosome missegregation in Ipl1 nuclear–depleted cells (Fig. 3, E–G). In meiosis I, 60% of Ipl1 nuclear–depleted cells displayed the uneven segregation phenotype, which was more penetrant than the cells with nuclear depletion of Bub3 (Fig. 2 E). Interestingly, in meiosis II, more than 80% of cells in which Ipl1 was depleted from the nucleus displayed an uneven segregation phenotype, which was similar to cells with nuclear depletion of Bub3. These results suggest that the uneven chromatin segregation phenotype in cells depleted of Bub3 is likely due to a loss of error correction by Ipl1, such that most chromosomes segregate to one spindle pole.

To test our hypothesis that kinetochore-localized Ipl1 levels were not sufficient to release aberrant kinetochore–microtubule attachments in meiosis without Bub3, we asked whether chromatin segregation is biased toward the old SPB, a phenotype observed in Ipl1-depleted cells (Meyer et al., 2013; Monje-Casas et al., 2007; Tanaka et al., 2002; Yu and Koshland, 2007). We tagged Spc42 with RedStar, a slower maturing RFP. When SPBs initially separate, the old SPB will be brighter than the new SPB until RedStar fully matures (Knop et al., 2002; Meyer et al., 2013). We tagged *HTB2* with GFP and assessed whether the larger DNA mass segregated to the old (bright) SPB or the new (dim) SPB (Fig. 4, A–E). We only scored cells with uneven chromatin segregation. With Bub3, Bub1, or Ipl1 nuclear depletion, the larger DNA mass segregates to the old SPB in >88% of cells in meiosis I and II (Fig. 4 F).

To further test the premise that kinetochores are unable to release improper initial attachments, we monitored a single homologous chromosome pair. We tagged the two homologous chromosome IVs with LacO near the centromere in cells expressing GFP-LacI and Spc42-RedStar (Robinett et al., 1996; Straight et al., 1996). We then used 3-min intervals for time-lapse microscopy and followed the location of the chromosome with respect to the SPBs (Fig. 5, A–E). We found three different patterns. First, the GFP focus was between the two SPBs and then properly segregated, suggesting that the chromosomes were bioriented before segregation. Second, the GFP focus stayed associated with one SPB and missegregated, suggesting that the chromosome was unable to undergo error correction and maintained the initial attachments. Third, the GFP focus traversed back and forth between the SPBs and missegregated, suggesting that the chromosome was undergoing error correction but unable to make proper attachments. In wild-type cells, almost all GFP foci were between the two SPBs and then properly segregated in both meiotic divisions (Fig. 5, A and B). With Ipl1 nuclear depletion, 96% of the GFP foci stayed attached to one SPB and did not traverse in meiosis I, similar to results from a previous study using a mutant allele of *IPL1* (Meyer et al., 2013). In meiosis II, 95% stayed attached to one SPB, suggesting that initial attachments were unable to correct (Fig. 5, A and C). With Bub3 nuclear depletion, 72% of GFP foci were between the two SPBs and properly segregated in meiosis I, 24% stayed attached to one SPB and missegregated, and only 4% traversed and missegregated. In meiosis II, 72% of GFP foci stayed attached to one SPB (Fig. 5, A, D, and E). These results support the conclusion that, upon Bub3 nuclear depletion, error-correction mechanisms, which release improper kinetochore–microtubule attachments, are not properly functioning in a fraction of cells in meiosis I and most cells in meiosis II. However, in both phases of

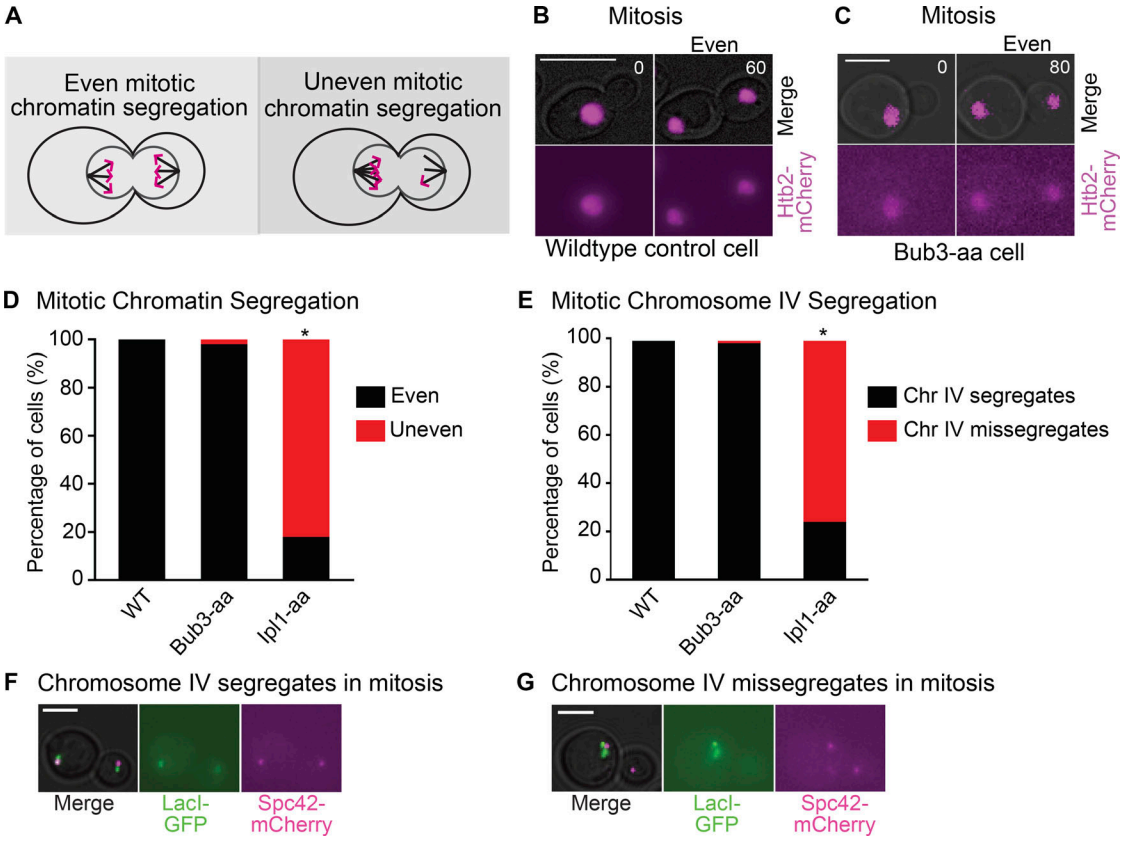

Figure 3. **Cells with nuclear depletion of Bub3 do not display massive chromatin missegregation in mitosis. (A)** Schematic of even and uneven chromatin segregation in mitosis. **(B and C)** Representative time lapses of wild-type cells (B) and cells with nuclear depletion of Bub3 (C; Bub3-aa) displaying even chromatin segregation in mitosis. Cells express Htb2-mCherry to visualize chromatin. Scale bars, 5 µm. **(D)** Percentage of cells that display even and uneven chromatin segregation in mitosis. At least 100 cells from two or more independent experiments per genotype. Asterisk indicates a statistically significant difference compared with the wild-type cells (*, P < 0.05, two-tailed Fisher's exact test). **(E)** Percentage of cells that displays proper and missegregation of a tagged chromosome IV in mitosis. At least 1,000 cells from two or more independent experiments per genotype. Asterisk indicates a statistically significant difference compared with the wild-type cells (*, P < 0.05, two-tailed Fisher's exact test). **(F and G)** Representative time lapse of a mitotic division in cells with nuclear depletion of Ipl1 (Ipl1-aa) showing proper segregation (F) and missegregation (G) of chromosome IV. Chromosome IV is marked with LacO in cells expressing LacI-GFP. aa, anchor away. Scale bars, 5 µm.

meiosis, Ipl1 nuclear depletion has a more penetrant defect than Bub3 nuclear depletion, suggesting that a low level of Ipl1 is active at the kinetochore in the absence of Bub3.

In mitosis, there are four known Ipl1 kinetochore recruitment pathways, in which one pathway is Bub3–Bub1–Sgo1 dependent (Cho and Harrison, 2011; Edgerton et al., 2016; Fischböck-Halwachs et al., 2019; Garcia-Rodriguez et al., 2019; Kawashima et al., 2010; Peplowska et al., 2014; Verzijlbergen et al., 2014; Yoon and Carbon, 1999). We hypothesize that the Bub3–Bub1–Sgo1 recruitment pathway is crucial for full Ipl1 kinetochore localization and/or maintenance in meiosis. In support of this hypothesis, previous work showed less-concentrated levels of Ipl1 at centromeres in the absence of Bub1 in meiosis by immunofluorescence (Yu and Koshland, 2007). We measured the levels of Ipl1-3GFP that colocalized with the kinetochore protein Mtw1-mRuby2. Because Ipl1-3GFP also localizes to spindle microtubules, we measured the levels at telophase I, after anaphase I spindle breakdown and just before the start of meiosis II (Fig. 6 A). We found that Ipl1 levels were reduced by 87% with Bub3 depletion (Fig. 6 B). In mitosis, the Ipl1 levels with Bub3 depletion were similar to those without Bub3 depletion (Fig. 6, C and D). Overall, our results suggested that the Bub3–Bub1–Sgo1 recruitment pathway is important for maintaining Ipl1 kinetochore levels in meiosis.

Premature PP1 kinetochore localization advances anaphase I and II onset

We hypothesized that the reduced levels of Ipl1 at the kinetochore in Bub3-, Bub1-, or Sgo1-depleted cells could also contribute to premature anaphase onset. To test this hypothesis, we measured the duration from SPB separation to anaphase I or II onset in cells depleted of Ipl1 at meiotic entry. We found that both metaphase I and II were shorter with Ipl1 depletion than in the wild-type control cells, similar to cells depleted of Bub3, Bub1, or Sgo1 (Fig. 1 C).

Previous work showed that complete loss of Ipl1 in meiosis, due to a meiotic null allele of *IPL1*, results in premature spindle formation in prophase I (Kim et al., 2013; Newnham et al., 2013; Shirk et al., 2011). To determine if premature spindle formation also occurs with Ipl1 anchored away at meiotic entry, we

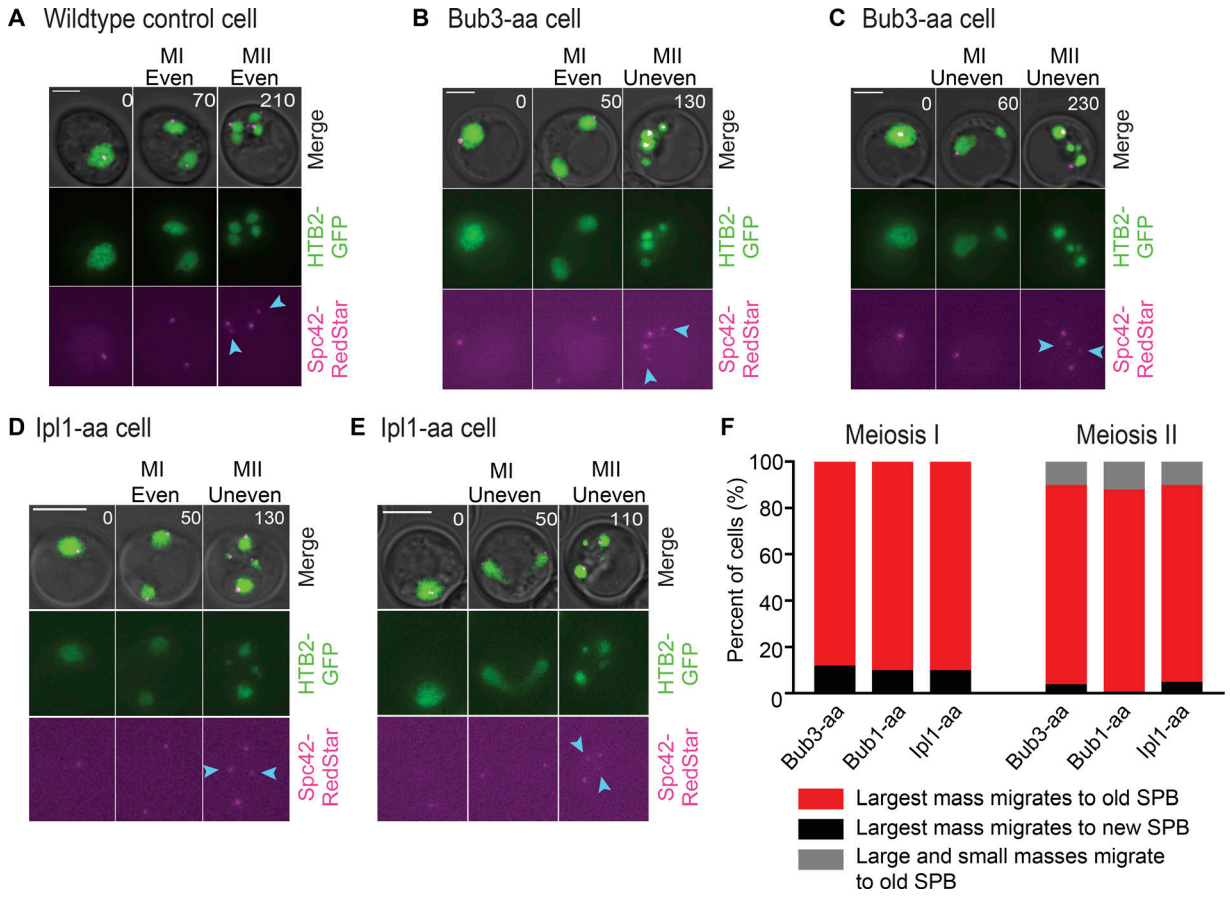

Figure 4. **Chromatin that missegregates in Bub3-depleted cells mostly migrates to the older SPB, similar to Ipl1-depleted cells. (A–E)** Representative time lapses of wild-type cells (A), cells with nuclear depletion of Bub3 (B and C), and Ipl1 (D and E) expressing Htb2-GFP and Spc42-RedStar. Time 0 marks prophase I. Scale bars, 5 µm. Arrowheads mark the dimmer (new) SPBs. **(F)** Percentage of cells in which the largest DNA masses migrate to the brighter (old) SPB in the first and second meiotic division. At least 100 cells from two or more independent experiments per genotype were analyzed. aa, anchor away.

monitored cells arrested at prophase I due to a deletion of *NDT80* and that expressed Spc42-mCherry, Tub1-GFP, and Zip1-GFP. We found that 94% of cells with Ipl1 anchored away displayed only a single SPB and lacked spindle formation in prophase I (Fig. S4). Wild-type cells and cells in which Bub3 was anchored away did not prematurely separate SPBs and did not form spindles in prophase I. These results suggest that the role of Ipl1 in blocking premature spindle formation does not require kinetochore localization. Furthermore, these results demonstrate that SPB separation occurs in prometaphase I in Ipl1-depleted cells, as it does Bub3-depleted cells. Therefore, our measured durations represent the time from prometaphase I to anaphase I onset in both Ipl1- and Bub3-depleted cells.

At the kinetochore, Ipl1 kinase activity and PP1 phosphatase activity counteract one another (Emanuele et al., 2008; Francisco et al., 1994; Hsu et al., 2000; Pinsky et al., 2009). In mammalian cells, Aurora B phosphorylates the PP1 binding site, weakening the interaction between PP1 and KNL1 (Liu et al., 2010). Once kinetochores are bioriented, Aurora B activity at the kinetochore decreases and PP1 binds KNL1 to reverse the phosphorylations on Aurora B substrates. Because PP1 can regulate the normal timing of mitotic progression (Kim et al., 2017; Suzuki et al., 2018), we hypothesized that reduced Ipl1 kinetochore localization in Bub3-depleted meiotic cells could lead to premature PP1 localization and activity at the kinetochore. To determine if premature PP1 localization leads to shorter metaphase in Bub3-depleted cells, we disrupted a kinetochore-binding site for Glc7, the catalytic subunit of PP1. Mutation of the Spc105/KNL1 RVSF motif to RASA disrupts checkpoint silencing, a major function of PP1 at the kinetochore, suggesting that PP1 is not present for checkpoint silencing (Hendrickx et al., 2009; Liu et al., 2010; Rosenberg et al., 2011). Because the *SPC105*^{RASA} mutants are lethal due to a failure to silence the checkpoint, we engineered strains such that wild-type Spc105 was present in mitosis and Spc105^{RASA} was present in meiosis when Bub3 was anchored away. We tagged both *SPC105* and *BUB3* with FRB in our anchor-away strain background and then integrated a copy of *SPC105*^{RASA} under the meiosis-specific *REC8* promoter at another locus. Addition of rapamycin depleted both wild-type Spc105 and Bub3, while cells produced Spc105^{RASA} in meiosis, allowing us to monitor the timings of the meiotic divisions in cells lacking Bub3 but expressing *SPC105*^{RASA}. To perform this experiment, we added rapamycin 7 h after resuspension into sporulation medium to allow for enough Spc105^{RASA} protein production before anchoring away the wild-type Spc105-FRB protein and

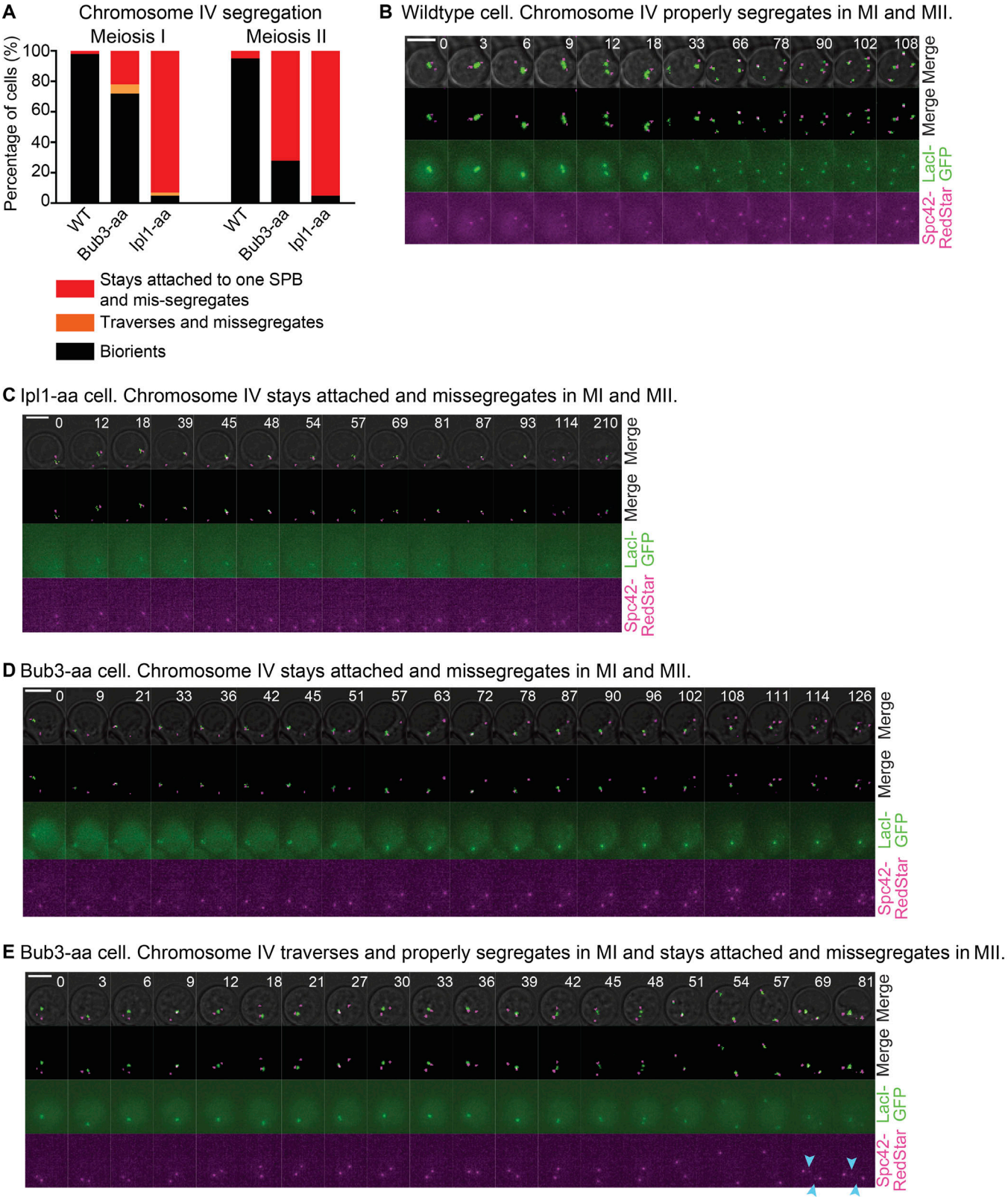

Figure 5. **Chromosome IV usually stays attached to one SPB when it missegregates in cells with nuclear depletion of Bub3. (A)** Percentage of cells classified in the indicated categories according to chromosome IV segregation behavior in the first and second meiotic divisions. At least 100 cells from three or more independent experiments per genotype were analyzed. **(B–E)** Representative time lapses of a wild-type cell (B), a cell with nuclear depletion of Ipl1 (C), or Bub3 (D and E). Arrowheads mark the dimmer (new) SPBs. These cells contain LacO repeats near the centromere of chromosome IV and express LacI-GFP and Spc42-RedStar. Time 0 marks metaphase I. Scale bars, 5 µm; aa, anchor away.

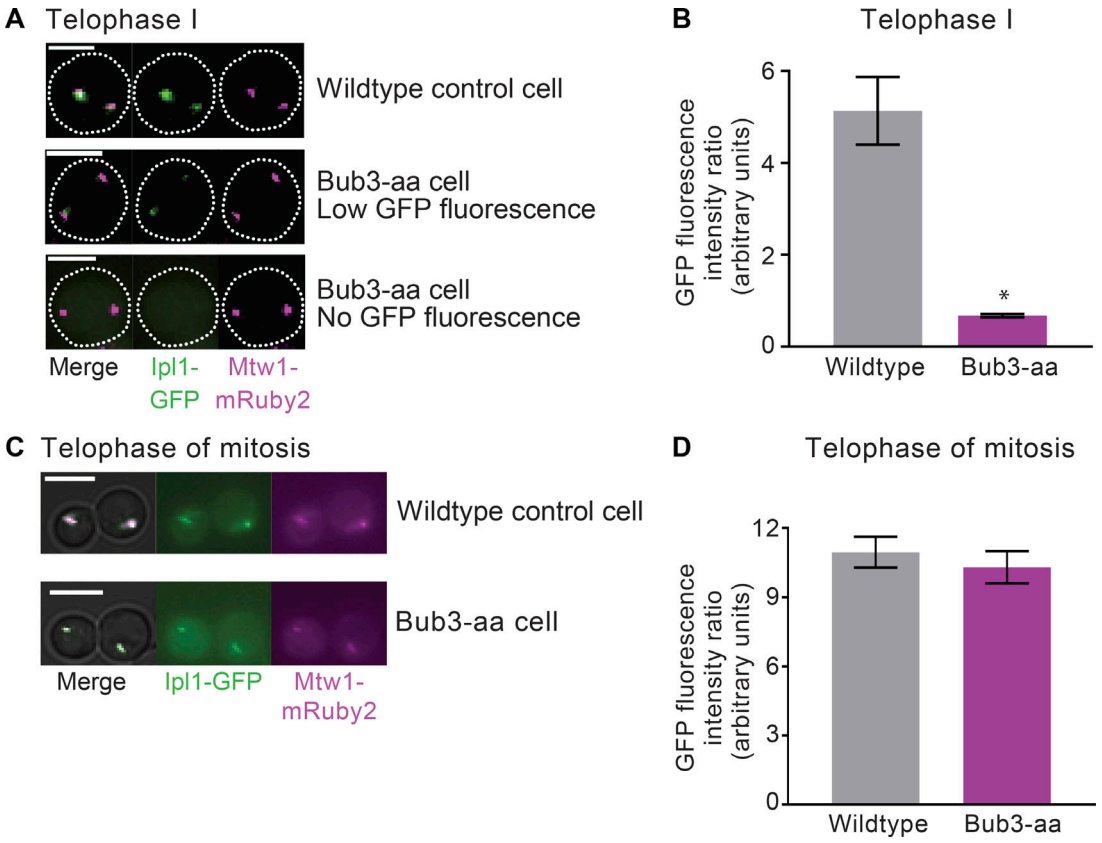

Figure 6. **Bub3-depleted cells have reduced kinetochore-localized Ipl1 levels in telophase I of meiosis but similar levels in telophase of mitosis. (A)** Representative images of wild-type cells and cells with nuclear depletion of Bub3 at telophase I. Cells express Ipl1-GFP and Mtw1-mRuby2 to visualize the kinetochore. Scale bars, 5 µm. **(B)** Graph showing the mean of Ipl1-GFP fluorescence intensity that colocalizes with kinetochore protein Mtw1-mRuby2 in wild-type cells and cells depleted of nuclear Bub3. Values plotted correspond to the ratio between Ipl1-GFP and Mtw1-mRuby2 fluorescence intensity at each Mtw1-mRuby2 spot; fluorescence background levels were subtracted for both channels. Error bars represent SEM. At least 100 cells from two or more independent experiments per genotype were monitored. Asterisk indicates a statistically significant difference compared with wild-type cells (*, $P < 0.05$, Mann-Whitney test). **(C)** Representative images of wild-type cells and cells with Bub3 nuclear depletion at telophase of mitosis. Cells express Ipl1-GFP and Mtw1-mRuby2 to visualize the kinetochore. Scale bars, 5 µm. **(D)** Graph showing the mean of Ipl1-GFP fluorescence intensity that colocalizes with kinetochore protein Mtw1-mRuby2 in wild-type cells and cells depleted of nuclear Bub3. Values plotted correspond to the ratio between Ipl1-GFP and Mtw1-mRuby2 fluorescence intensity at each Mtw1-mRuby2 spot; fluorescence background levels were subtracted for both channels. Error bars represent SEM. At least 100 cells from two or more independent experiments per genotype were monitored. aa, anchor away.

Bub3-FRB. We then only analyzed cells that underwent the first meiotic division within 2–3 h of rapamycin addition, suggesting that they were in prophase I at the time of rapamycin addition. As a control, we integrated wild-type *SPC105* under the *REC8* promoter and performed the same analysis.

We found that the control cells depleted of both Bub3 and Spc105 in prophase I but expressing the wild-type *SPC105* have a premature anaphase I and II onset, similar to the cells depleted of Bub3 at meiotic initiation (Fig. 7 A). This result reinforces the model that Bub3 is acting only during chromosome segregation and is not an indirect consequence of defects earlier in meiosis. In cells depleted of both Bub3 and Spc105 in prophase I but expressing *SPC105*^{RASA}, anaphase I and II onset occurred with similar timings to wild-type cells (Fig. 7 A). These results suggest that preventing premature PP1 kinetochore localization by mutating the PP1 binding site on the Spc105 receptor rescues the normal timing of anaphase I and II onset.

To further test whether the rescue in the time of anaphase onset of Bub3-depleted cells expressing *SPC105*^{RASA} was due to the loss of PP1 localization, we asked if fusion of *GLC7* to *SPC105*^{RASA} could prevent the rescue. We used a strain with a fusion protein of *GLC7* tethered to *SPC105*^{RASA} (Rosenberg et al., 2011) and crossed it into our *BUB3-FRB* anchor-away background. In these cells, both anaphase I and anaphase II onset were faster, similar to cells depleted of Bub3, suggesting that bringing Glc7 back to the kinetochore prevented the rescue of the timings by Spc105^{RASA} (Fig. 7 A). In cells wherein *GLC7* was tethered to *SPC105*^{RASA} but without the depletion of Bub3, meiosis I and II were slower when compared with the same cells with Bub3 depleted; however, both phases were faster than wild-type cells (Fig. S5). Overall, these results support our hypothesis that premature PP1 localization in Bub3-depleted cells results in faster anaphase onset.

Finally, we asked if premature PP1 kinetochore localization, in an otherwise wild-type cell, could also result in faster anaphase onset. We mutated the RVSF motif on Spc105 to RVAF. The Spc105^{RVAF} cannot be phosphorylated by Ipl1 and therefore should allow PP1 to bind prematurely (Hendrickx et al., 2009;

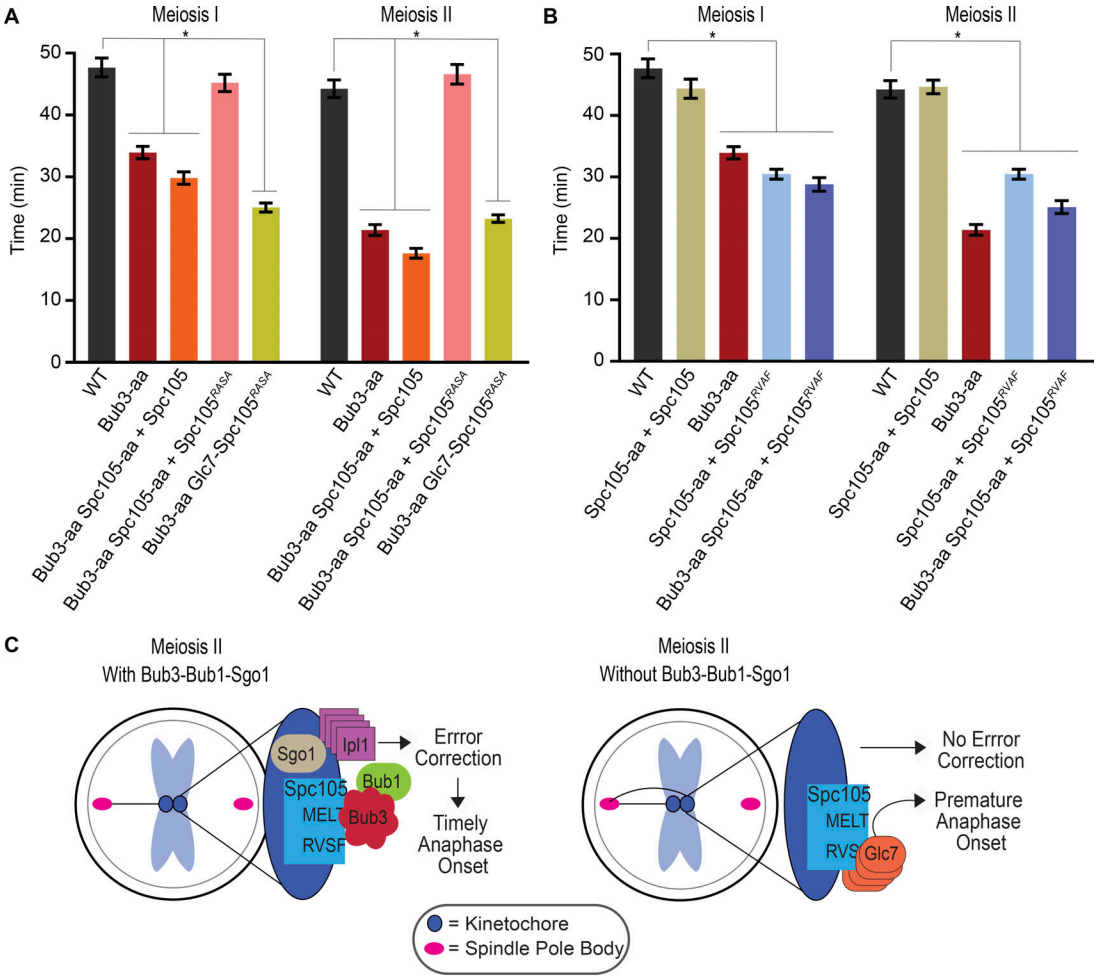

Figure 7. **Bub3 regulates the Ipl1/PP1 balance at the kinetochore, ensuring proper anaphase onset and chromosome segregation. (A)** Graph of wild-type cells, cells with nuclear depletion of Bub3, and cells with nuclear depletion of Bub3 and Spc105. Those that have a nuclear depletion of Spc105 also express *SPC105* or *SPC105*^{RASA}, under the meiosis-specific *REC8* promoter, at the *TRP1* or *LEU2* locus. Rapamycin was added 7 h after the cells were resuspended in sporulation medium. Error bars represent SEM. At least 100 cells from two or more independent experiments per genotype were monitored. Asterisks indicate a statistically significant difference compared with wild-type cells (*, P < 0.05, Mann-Whitney test). **(B)** Graph of wild-type cells with nuclear depletion of Spc105 and cells with nuclear depletion of Bub3. Cells with nuclear depletion of Spc105 express *SPC105* or *SPC105*^{RVAF} under the REC8 promoter for meiosis-specific expression, localized at the *TRP1* or *LEU2* locus. Cells expressing *GLC7-SPC105*^{RASA} produce a fusion protein of Glc7 and Spc105 under the control of the *SPC105* promoter at the endogenous locus. Error bars represent SEM. At least 100 cells from two or more independent experiments per genotype were monitored. Asterisks indicate a statistically significant difference compared with wild-type cells (*, P < 0.05, Mann-Whitney test). **(C)** Model: Bub3 recruits and maintains Ipl1 at the kinetochore, which ensures proper meiotic chromosome segregation. This prevents PP1 from prematurely binding the kinetochore and premature APC/C activation, which ensures proper anaphase onset. aa, anchor away.

Liu et al., 2010; Rosenberg et al., 2011). We anchored away the wild-type Spc105 and expressed either *SPC105* or *SPC105*^{RVAF} from the *REC8* promoter. Expression of *SPC105* showed the normal timing of anaphase I and II onset (Fig. 7 B). In contrast, expression of *SPC105*^{RVAF} resulted in premature anaphase I and II onset (Fig. 7 B). Anchoring away Bub3 did not further decrease the time to anaphase I and II onset. These results support our hypothesis that premature PP1 localization can indeed lead to faster anaphase onset. It is interesting to note that the *SPC105*^{RVAF} strain did not lead to a faster mitotic anaphase, suggesting another difference between meiotic and mitotic regulation (Rosenberg et al., 2011). Overall, we conclude that cells depleted of Bub3 have less Ipl1 at the kinetochore, leading to premature PP1 localization and faster anaphase onset (Fig. 7 C).

Discussion

Many mitotic cell cycle regulators often have modified functions in meiosis important for the meiotic chromosome segregation program. A noteworthy example of a regulatory pathway with increased roles in meiosis is the spindle checkpoint. In addition to delaying anaphase onset if chromosomes are not attached to spindle microtubules, individual spindle checkpoint proteins also have specialized regulatory functions in meiosis. In *Caenorhabditis elegans*, spindle checkpoint proteins MAD-1, MAD-2, and BUB-3 have adopted another function in that they are required for the synapsis checkpoint, which induces apoptosis if cells have not assembled synaptonemal complex during prophase I (Bhalla and Dernburg, 2005; Bohr et al., 2015). The synapsis checkpoint mechanism does not rely on the inhibition

of APC/C activity, suggesting that the spindle checkpoint proteins evolved a novel mechanism of action. In another example, the spindle checkpoint protein Mad2 has a more important role in meiosis than in mitosis in regulating chromosome segregation in *Saccharomyces cerevisiae*. Deletion of *MAD2* in mitosis does not have any major consequence (Li and Murray, 1991). In contrast, in meiosis, *mad2Δ* cells have enhanced chromosome missegregation in meiosis I and premature anaphase I onset, likely due to premature APC/C activity (Shonn et al., 2000; Shonn et al., 2003; Tsuchiya et al., 2011). Mad1 and Mad2 have roles in biorientation (Shonn et al., 2003). Loss of Mad3 in meiosis does not cause similar phenotypes, although Mad3 is required for spindle checkpoint signaling and for homeologous chromosome segregation (Cheslock et al., 2005).

In this study, we show that the spindle checkpoint proteins Bub1 and Bub3 also have more important checkpoint-independent functions in meiosis compared with mitosis. Meiotic nuclear depletion of Bub1 or Bub3 causes a shorter metaphase I and II. This is in contrast to the results in mitosis in which *bub1Δ* and *bub3Δ* cells have a delayed anaphase onset (Kim et al., 2015; Yang et al., 2015). In addition, we show that Bub1 and Bub3 are crucial in meiosis for regulating bipolar kinetochore–microtubule attachments for proper chromosome segregation. Loss of *BUB1* or *BUB3* in meiosis, either through anchor away or through a deletion allele, causes massive chromosome missegregation in meiosis II, in which most chromosomes segregate to one spindle pole and <1% of the spores are viable (Fig. 4, E and F; and Fig. S2 B). In mitosis, *bub1Δ* and *bub3Δ* cells are viable (Hoyt et al., 1991) and have a low chromosome missegregation rate of <2% per division (Fig. 3 E).

Massive chromosome missegregation, in which most chromosomes are pulled to one spindle pole, was a phenotype originally discovered in mitosis with a temperature-sensitive mutation in the Ipl1 kinase (Tanaka et al., 2002). It is now understood that Ipl1 phosphorylates outer kinetochore proteins to release kinetochore–microtubule attachments that are not under tension, allowing another attempt to make proper attachments (Biggins and Murray, 2001; Cheeseman et al., 2002; Kang et al., 2001; Li et al., 2002; London et al., 2012; Tanaka et al., 2002; Tien et al., 2010). In addition, Ipl1 is required for spindle checkpoint signaling of tensionless attachments, likely by disrupting kinetochore–microtubule attachments. Therefore, cells that lack Ipl1 cannot correct improper microtubule–kinetochore attachments, and they are unable to signal the spindle checkpoint. In both mitosis and meiosis, the initial attachments of kinetochores mainly occur from microtubules emanating from the old, more mature SPB, such that loss of Ipl1 results in uneven segregation of chromosomes, with the majority of chromosomes traveling to the old SPB (Meyer et al., 2013; Tanaka et al., 2002).

Previous work showed that Bub1 has a role in recruiting Ipl1 to the kinetochore in both mitosis and meiosis (Kawashima et al., 2007; Kawashima et al., 2010; Peplowska et al., 2014; Verzijlbergen et al., 2014; Yu and Koshland, 2007). However, massive chromosome missegregation does not occur in the absence of *BUB1* and *BUB3* in mitosis, likely because there are three other known pathways responsible for bringing Ipl1 to the kinetochore in addition to the Bub3–Bub1 pathway (Cho and Harrison, 2011; Edgerton et al., 2016; Fischböck-Halwachs et al., 2019; Garcia-Rodriguez et al., 2019; Yoon and Carbon, 1999). Interestingly, we find that with the depletion of Bub1 or Bub3, massive chromosome missegregation was more penetrant in meiosis II than in meiosis I (Fig. 2, E–G). We note that although there were fewer cells with massive chromosome missegregation in meiosis I, aneuploidy still occurred. Tagging an individual chromosome IV showed that Bub3-depleted cells missegregated this chromosome in 28% of meiosis I divisions (Fig. 5 A), similar to previous reports with *BUB3*-deleted cells (Marston et al., 2004). These results suggest that, although there is enough Ipl1 for most cells to undergo initial rounds of error correction in meiosis I, there is not enough Ipl1 to prevent all chromosome missegregation. In meiosis II, our results suggest that, when Bub1 or Bub3 is depleted, most cells are unable to undergo even the initial rounds of error correction leading to massive chromosome missegregation in which most chromosomes travel to the old SPB (Figs. 2, E–G; 4 F, and 5 A).

Why is chromosome missegregation more penetrant in meiosis II than meiosis I or mitosis, when Bub1, Bub3, or Sgo1 is depleted? Ipl1levels in mitotic telophase are similar in wild-type cells and cells depleted of Bub3 (Fig. 6 D). Mitotic cells lacking Bub1 or Bub3 likely have enough Ipl1 at the kinetochore, recruited through the other recruitment pathways, to undergo multiple rounds of error correction, which prevents massive chromosome missegregation. Meiotic cells lacking Bub1 or Bub3 likely have sufficient levels of Ipl1 for a couple of rounds of error correction during metaphase I. However, Ipl1 kinetochore levels were substantially reduced in telophase I (Fig. 6 B). Because metaphase II is much faster in the Bub1- or Bub3-depleted cells, it is likely that there is insufficient time for error correction of kinetochores with low levels of Ipl1 (Fig. 1, A–C). Another possibility is that redundant mechanisms occur for recruitment of Ipl1 in meiosis I, but not in meiosis II.

Our findings that depletion of Bub1, Bub3, or Sgo1 resulted in a shorter duration of metaphase I and II onset were surprising. We previously showed that loss of *BUB1* and *BUB3* in mitosis displayed the opposite phenotype, a delayed anaphase onset (Yang et al., 2015). However, meiotic cells had a substantially lower level of kinetochore-localized Ipl1, leading us to test whether disruptions in the balance between Ipl1 kinase and its counteracting phosphatase PP1 led to a shorter metaphase. We found that cells depleted of Ipl1 also had a shorter duration to anaphase onset (Fig. 1 C). Furthermore, disruption of the PP1-binding site on kinetochore protein Spc105 rescued the shorter metaphase phenotype of Bub3-depleted cells (Fig. 7 A). Tethering the PP1 catalytic subunit to $Spc105^{RASA}$ disrupted the rescue. These results suggest that the balance between Ipl1 and PP1 at the kinetochore sets the duration of meiosis such that premature PP1 binding leads to a shorter metaphase I and II onset. Understanding which Ipl1 and PP1 substrates regulate meiotic progression is an important future direction. Our results support the model that recruitment of Ipl1 through Bub3–Bub1 is essential for maintaining Ipl1 levels for error correction and preventing PP1 kinetochore localization until chromosomes have properly attached to spindle microtubules during meiosis (Fig. 7 C).

Materials and methods

Strains and manipulations

Strains used in this study are derivatives of *S. cerevisiae* W303 (Table S1). Gene tagging and deletions were performed using standard PCR-based transformations (Janke et al., 2004; Longtine et al., 1998). Any manipulations were verified by PCR. The anchor-away strains were built in strain backgrounds previously described but with *BUB3*, *BUB1*, *SGO1*, *IPL1*, or *SPC105* tagged with FRB at the endogenous locus and RPL13A with 2XFKBP12 (Haruki et al., 2008). The $SPC105^{RASA}$ and $SPC105^{RVAF}$ strains were made by first cloning *SPC105* under the *REC8* promoter into a yeast integrating plasmid, using site-directed mutagenesis to mutate the RVSF motif and then integrating the plasmid into the *TRP1* or *LEU2* locus. The *GlLC7-SPC105*^{RASA} strain was engineered previously and crossed into the anchor-away strains (Rosenberg et al., 2011).

Growth conditions

For all the meiotic experiments except the $P_{GAL1,10}$-*NDT80 Gal4-ER* and *ndt80Δ* experiments, cells were grown overnight in YPD (1% yeast extract, 2% peptone, and 2% dextrose) at 30°C, transferred with a 1:40 dilution to YPA (1% yeast extract, 2% peptone, and 1% potassium acetate) for 12–16 h at 30°C, washed twice with water, and then incubated in 1% potassium acetate at 25°C for 7–8 h. In all experiments with nuclear depletion, except for cells wherein Bub3 was depleted at prophase I (as mentioned in text) and cells expressing $P_{GAL1,10}$-*NDT80 Gal4-ER*, rapamycin (1 µg/ml) was added at the same time cells were transferred to potassium acetate. To deplete Bub3 at prophase I, rapamycin (1 µg/ml) was added after 7 h of transferring the cells to potassium acetate; only cells in prophase I at the time of rapamycin addition were analyzed. In the $P_{GAL1,10}$-*NDT80 Gal4-ER* experiments, cells were grown overnight in YPD at 30°C and transferred with a 1:40 dilution to YPA for 12–16 h at 30°C; cells were transferred to potassium acetate for 10–11 h to allow the cells to reach a prophase I arrest; after β-estradiol addition (1 µM; Sigma) and with or without rapamycin (1 µg/ml) addition, time-lapse microscopy was used to image these cells during the second meiotic division. Cells containing *ndt80Δ* were incubated in YPD at 30°C and transferred with a 1:40 dilution to YPA for 12–16 h at 30°C; after 10–11 h in sporulation media, cells were imaged. For mitosis experiments, cells were grown in 2× synthetic complete medium (0.67% bacto–yeast nitrogen base without amino acids, 0.2% dropout mix with all amino acids, and 2% glucose) overnight at 30°C and then diluted and grown to log phase for assessment.

Microscope image acquisition and time-lapse microscopy

All movies were performed in a chamber mounted on a coverslip coated with Concanavalin A (Sigma). In all meiosis movies, except the movies corresponding to the $P_{GAL1,10}$-*NDT80 Gal4-ER* experiments, after 6–8 h of transferring cells to potassium acetate, cells were concentrated and loaded into the coverslip in a chamber. An agar pad containing potassium acetate was used to create a monolayer of cells and removed before imaging; preconditioned potassium acetate medium was added. In the meiosis movies corresponding to the $P_{GAL1,10}$-*NDT80 Gal4-ER* experiments, cells were transferred into potassium acetate for 10–11 h instead of 6–8 h, but the movie preparations remained the same as in the other meiosis movies. In all mitosis movies, cells were grown overnight in 2× synthetic complete medium (0.67% bacto–yeast nitrogen base without amino acids, 0.2% dropout mix with all amino acids, and 2% glucose); rapamycin (1 µg/ml) was added to log phase cells 2–3 h before imaging.

Cells were imaged at room temperature using a Nikon Ti-E inverted-objective microscope equipped with a 60× oil objective (Plan Apochromat NA 1.4 oil), a Lambda 10–3 optical filter changer and Smartshutter, GFP and mCherry filters (Chroma Technology), and a charge-coupled device camera (CoolSNAP HQ2; Photometrics). During time-lapse imaging, Z stacks of five sections of 1.2 mm each were acquired at 10-min intervals with exposure times of 60–70 ms for bright field and 700–900 ms for GFP and mCherry with neutral-density filters transmitting 2–32% of light intensity. While meiosis movies were 12–13 h long, mitosis movies were 6–8 h long. Cells expressing Ipl1-GFP MTW1-mRuby2 as well as *ndt80Δ* cells were mounted (without fixation) on a coverslip and imaged every 10 min using 15 Z stacks (0.4 µm each) after being in potassium acetate for 9–11 h; cells in telophase I and mitotic telophase expressing Ipl1-GFP MTW1-mRuby2 were used for fluorescence intensity measurements.

Cells producing Htb2-mCherry, Spc42-RedStar and Htb2-GFP, LacI-GFP and Spc42-mCherry, or Bub3-FRB-GFP were imaged at room temperature using a DeltaVision pDV microscope (Applied Precision) equipped with a CoolSNAP HQ2/HQ2-ICX285 camera using a 60× oil objective (U-Plan S-Apochromat-N, 1.4 NA). Images were acquired using SoftWoRx software (GE Heathcare). During time-lapse imaging, five Z steps (0.8 µm) were acquired every 10 min for 12 h except for cells expressing LacI-GFP, wherein images were acquired every 3 min for 10–12 h. The exposure times used to image bright field, Htb2-mCherry, LacI-GFP, Spc42-mCherry, and Bub3-FRB-GFP were 0.3–0.4 ms, 0.02–0.03 ms, 0.3–0.4 ms, 0.4 ms, and 0.3–0.5 ms, respectively, with neutral-density filters transmitting 5–32% of light intensity.

Image processing

We processed all images using ImageJ (National Institutes of Health). Z stacks were combined into a single maximum intensity projection with NIS-Elements software (Nikon) to obtain the final images presented in this article. Brightness and contrast were adjusted on entire images only.

Quantification analysis

Images from cells expressing Htb2-mCherry were quantified using Imarisx64 Software. We measured the area (square micrometers) of each DNA mass after the first and second meiotic division by adding all the area values in each Z stack. To determine even and uneven DNA masses, we measured the DNA masses area after mitosis and the first and second meiotic division of our wild-type and anchor-away strains using Imarisx64. For each wild-type cell, after the mitotic or meiosis I division, the two DNA mass sizes were obtained and then subtracted from one another to get a mass size difference. For meiosis II cells, similar calculations were done with the four

DNA mass sizes. The resulting difference values were averaged and the SD was used to calculate a range of what we called "even" DNA masses (average ± SD). The same measurements and calculations were performed in the individual cells of the anchor-away strains; anything outside of the even range (of average ± SD) set by the wild-type cells was considered "uneven." These values were plotted using Prism (GraphPad Software).

Fluorescence intensity

To measure Ipl1-GFP fluorescence intensity at the kinetochore (using colocalization with kinetochore protein MTW1-mRuby2) of telophase I cells and mitotic telophase cells using ImageJ (Fiji) software, a circle was drawn around the MTW1-mRuby2 region and the sum intensity of the mRuby2 channel (M) and GFP channel (I) throughout the Z stacks were recorded. For background subtraction, the circle was moved to several regions not containing MTW1-mRuby2 nor Ipl1-GFP, and the sum intensity through the Z stacks was recorded for both mRuby2 ($M_{background}$) and GFP ($I_{background}$); the average of the background fluorescence for each channel was calculated and subtracted from each value above. To determine the fluorescence intensity of Ipl1-GFP at the kinetochore, we calculated the ratio between the Ipl1-GFP and MTW1-mRuby2 values as follows: $(I - I_{background})/(M - M_{background})$. All ratio values were averaged together and plotted using Prism (GraphPad Software).

Statistical analysis

Statistical analysis was performed using Prism (GraphPad Software). Statistical analysis for anaphase onset timing, fluorescence intensity, and the Bub3-FRB-GFP experiment was done using an unpaired, nonparametric Mann-Whitney test with computation of two-tailed exact P values. To analyze Cdc14 release and DNA masses (HTB2-mCherry strains) percentages, we used the two-sided Fisher's exact test. The number of data points (n) is indicated in the figure legends. Statistically significant differences (P value <0.05) are indicated with an asterisk.

Spotting assay

Spot-test series were 10-fold serial dilutions from saturated overnight cultures. Dilution series were spotted on YPD (1% bacto–yeast extract, 2% bactopeptone, and 2% glucose), YPD + rapamycin (1 µg/ml), YPD + benomyl (15 µg/ml), and YPD + rapamycin (1 µg/ml) + benomyl (15 µg/ml). The plates were incubated at 30°C for 36–40 h before imaging.

Online supplemental material

Fig. S1 shows control experiments demonstrating that the anchor-away system removes Bub3-GFP-FRB from the nucleus and causes phenotypes similar to the deletion strains when Bub3, Bub1, or Sgo1 is depleted. Fig. S2 shows that the anchor away of Bub3, Bub1, Sgo1, or Ipl1 causes a loss of spore viability. Fig. S3 shows that Cdc14 release occurs at the time of spindle elongation in wild-type cells and cells depleted of Bub3. Fig. S4 shows that wild-type cells and cells depleted of Bub3, Bub1, and Ipl1 rarely form premature spindles in prophase I. Fig. S5 shows control experiments for Fig. 7 A in which rapamycin was or was not added to cells expressing *BUB3-FRB* and *SPC105*^{RASA} fused with *GLC7* under the *SPC105* promoter. Table S1 shows the budding yeast strains used.

Acknowledgments

We thank Andreas Hochwagen and Fred Cross for strains. We thank Frank Solomon and members of the Lacefield and Pelisch laboratories for insightful comments on the manuscript. We thank Jim Powers and the Light Microscopy Imaging Center at Indiana University.

This work was supported by a grant from the National Institutes of Health (GM105755).

The authors declare no competing financial interests.

Author contributions: S. Lacefield and G. Cairo conceived the project and wrote the manuscript. G. Cairo and A.M. MacKenzie constructed strains, performed the experiments, and analyzed the data. S. Lacefield, G. Cairo, and A.M. MacKenzie designed the experiments. All authors edited the final paper.

Submitted: 21 September 2019
Revised: 2 January 2020
Accepted: 15 January 2020

References

Benjamin, K.R., C. Zhang, K.M. Shokat, and I. Herskowitz. 2003. Control of landmark events in meiosis by the CDK Cdc28 and the meiosis-specific kinase Ime2. *Genes Dev.* 17:1524–1539. https://doi.org/10.1101/gad.1101503

Bhalla, N., and A.F. Dernburg. 2005. A conserved checkpoint monitors meiotic chromosome synapsis in Caenorhabditis elegans. *Science.* 310: 1683–1686. https://doi.org/10.1126/science.1117468

Biggins, S., and A.W. Murray. 2001. The budding yeast protein kinase Ipl1/Aurora allows the absence of tension to activate the spindle checkpoint. *Genes Dev.* 15:3118–3129. https://doi.org/10.1101/gad.934801

Bohr, T., C.R. Nelson, E. Klee, and N. Bhalla. 2015. Spindle assembly checkpoint proteins regulate and monitor meiotic synapsis in C. elegans. *J. Cell Biol.* 211:233–242. https://doi.org/10.1083/jcb.201409035

Bullitt, E., M.P. Rout, J.V. Kilmartin, and C.W. Akey. 1997. The yeast spindle pole body is assembled around a central crystal of Spc42p. *Cell.* 89: 1077–1086. https://doi.org/10.1016/S0092-8674(00)80295-0

Carlile, T.M., and A. Amon. 2008. Meiosis I is established through division-specific translational control of a cyclin. *Cell.* 133:280–291. https://doi.org/10.1016/j.cell.2008.02.032

Carminati, J.L., and T. Stearns. 1997. Microtubules orient the mitotic spindle in yeast through dynein-dependent interactions with the cell cortex. *J. Cell Biol.* 138:629–641. https://doi.org/10.1083/jcb.138.3.629

Cheeseman, I.M., S. Anderson, M. Jwa, E.M. Green, J. Kang, J.R. Yates III, C.S. Chan, D.G. Drubin, and G. Barnes. 2002. Phospho-regulation of kinetochore-microtubule attachments by the Aurora kinase Ipl1p. *Cell.* 111:163–172. https://doi.org/10.1016/S0092-8674(02)00973-X

Cheslock, P.S., B.J. Kemp, R.M. Boumil, and D.S. Dawson. 2005. The roles of MAD1, MAD2 and MAD3 in meiotic progression and the segregation of nonexchange chromosomes. *Nat. Genet.* 37:756–760. https://doi.org/10.1038/ng1588

Cho, U.S., and S.C. Harrison. 2011. Ndc10 is a platform for inner kinetochore assembly in budding yeast. *Nat. Struct. Mol. Biol.* 19:48–55. https://doi.org/10.1038/nsmb.2178

Edgerton, H., M. Johansson, D. Keifenheim, S. Mukherjee, J.M. Chacón, J. Bachant, M.K. Gardner, and D.J. Clarke. 2016. A noncatalytic function of the topoisomerase II CTD in Aurora B recruitment to inner centromeres during mitosis. *J. Cell Biol.* 213:651–664. https://doi.org/10.1083/jcb.201511080

Emanuele, M.J., W. Lan, M. Jwa, S.A. Miller, C.S. Chan, and P.T. Stukenberg. 2008. Aurora B kinase and protein phosphatase 1 have opposing roles in

modulating kinetochore assembly. *J. Cell Biol.* 181:241–254. https://doi.org/10.1083/jcb.200710019

Espeut, J., P. Lara-Gonzalez, M. Sassine, A.K. Shiau, A. Desai, and A. Abrieu. 2015. Natural Loss of Mps1 Kinase in Nematodes Uncovers a Role for Polo-like Kinase 1 in Spindle Checkpoint Initiation. *Cell Reports.* 12: 58–65. https://doi.org/10.1016/j.celrep.2015.05.039

Fischböck-Halwachs, J., S. Singh, M. Potocnjak, G. Hagemann, V. Solis-Mezarino, S. Woike, M. Ghodgaonkar-Steger, F. Weissmann, L.D. Gallego, J. Rojas, et al. 2019. The COMA complex interacts with Cse4 and positions Sli15/Ipl1 at the budding yeast inner kinetochore. *eLife.* 8:e42879. https://doi.org/10.7554/eLife.42879

Francisco, L., W. Wang, and C.S. Chan. 1994. Type 1 protein phosphatase acts in opposition to IpL1 protein kinase in regulating yeast chromosome segregation. *Mol. Cell. Biol.* 14:4731–4740. https://doi.org/10.1128/MCB.14.7.4731

García-Rodríguez, L.J., T. Kasciukovic, V. Denninger, and T.U. Tanaka. 2019. Aurora B-INCENP Localization at Centromeres/Inner Kinetochores Is Required for Chromosome Bi-orientation in Budding Yeast. *Curr. Biol.* 29:1536–1544.e4. https://doi.org/10.1016/j.cub.2019.03.051

Haruki, H., J. Nishikawa, and U.K. Laemmli. 2008. The anchor-away technique: rapid, conditional establishment of yeast mutant phenotypes. *Mol. Cell.* 31:925–932. https://doi.org/10.1016/j.molcel.2008.07.020

Hendrickx, A., M. Beullens, H. Ceulemans, T. Den Abt, A. Van Eynde, E. Nicolaescu, B. Lesage, and M. Bollen. 2009. Docking motif-guided mapping of the interactome of protein phosphatase-1. *Chem. Biol.* 16: 365–371. https://doi.org/10.1016/j.chembiol.2009.02.012

Hoyt, M.A., L. Totis, and B.T. Roberts. 1991. S. cerevisiae genes required for cell cycle arrest in response to loss of microtubule function. *Cell.* 66: 507–517. https://doi.org/10.1016/0092-8674(81)90014-3

Hsu, J.Y., Z.W. Sun, X. Li, M. Reuben, K. Tatchell, D.K. Bishop, J.M. Grushcow, C.J. Brame, J.A. Caldwell, D.F. Hunt, et al. 2000. Mitotic phosphorylation of histone H3 is governed by Ipl1/aurora kinase and Glc7/PP1 phosphatase in budding yeast and nematodes. *Cell.* 102:279–291. https://doi.org/10.1016/S0092-8674(00)00034-9

Indjeian, V.B., B.M. Stern, and A.W. Murray. 2005. The centromeric protein Sgo1 is required to sense lack of tension on mitotic chromosomes. *Science.* 307:130–133. https://doi.org/10.1126/science.1101366

Janke, C., M.M. Magiera, N. Rathfelder, C. Taxis, S. Reber, H. Maekawa, A. Moreno-Borchart, G. Doenges, E. Schwob, E. Schiebel, and M. Knop. 2004. A versatile toolbox for PCR-based tagging of yeast genes: new fluorescent proteins, more markers and promoter substitution cassettes. *Yeast.* 21:947–962. https://doi.org/10.1002/yea.1142

Kang, J., I.M. Cheeseman, G. Kallstrom, S. Velmurugan, G. Barnes, and C.S. Chan. 2001. Functional cooperation of Dam1, Ipl1, and the inner centromere protein (INCENP)-related protein Sli15 during chromosome segregation. *J. Cell Biol.* 155:763–774. https://doi.org/10.1083/jcb.200105029

Katis, V.L., J.J. Lipp, R. Imre, A. Bogdanova, E. Okaz, B. Habermann, K. Mechtler, K. Nasmyth, and W. Zachariae. 2010. Rec8 phosphorylation by casein kinase 1 and Cdc7-Dbf4 kinase regulates cohesin cleavage by separase during meiosis. *Dev. Cell.* 18:397–409. https://doi.org/10.1016/j.devcel.2010.01.014

Kawashima, S.A., T. Tsukahara, M. Langegger, S. Hauf, T.S. Kitajima, and Y. Watanabe. 2007. Shugoshin enables tension-generating attachment of kinetochores by loading Aurora to centromeres. *Genes Dev.* 21:420–435. https://doi.org/10.1101/gad.1497307

Kawashima, S.A., Y. Yamagishi, T. Honda, K. Ishiguro, and Y. Watanabe. 2010. Phosphorylation of H2A by Bub1 prevents chromosomal instability through localizing shugoshin. *Science.* 327:172–177. https://doi.org/10.1126/science.1180189

Kelly, A.E., C. Ghenoiu, J.Z. Xue, C. Zierhut, H. Kimura, and H. Funabiki. 2010. Survivin reads phosphorylated histone H3 threonine 3 to activate the mitotic kinase Aurora B. *Science.* 330:235–239. https://doi.org/10.1126/science.1189505

Kerrebrock, A.W., W.Y. Miyazaki, D. Birnby, and T.L. Orr-Weaver. 1992. The Drosophila mei-S332 gene promotes sister-chromatid cohesion in meiosis following kinetochore differentiation. *Genetics.* 130:827–841.

Kiburz, B.M., A. Amon, and A.L. Marston. 2008. Shugoshin promotes sister kinetochore biorientation in Saccharomyces cerevisiae. *Mol. Biol. Cell.* 19:1199–1209. https://doi.org/10.1091/mbc.e07-06-0584

Kim, S., R. Meyer, H. Chuong, and D.S. Dawson. 2013. Dual mechanisms prevent premature chromosome segregation during meiosis. *Genes Dev.* 27:2139–2146. https://doi.org/10.1101/gad.227454.113

Kim, T., M.W. Moyle, P. Lara-Gonzalez, C. De Groot, K. Oegema, and A. Desai. 2015. Kinetochore-localized BUB-1/BUB-3 complex promotes anaphase onset in C. elegans. *J. Cell Biol.* 209:507–517. https://doi.org/10.1083/jcb.201412035

Kim, T., P. Lara-Gonzalez, B. Prevo, F. Meitinger, D.K. Cheerambathur, K. Oegema, and A. Desai. 2017. Kinetochores accelerate or delay APC/C activation by directing Cdc20 to opposing fates. *Genes Dev.* 31: 1089–1094. https://doi.org/10.1101/gad.302067.117

Kitajima, T.S., S.A. Kawashima, and Y. Watanabe. 2004. The conserved kinetochore protein shugoshin protects centromeric cohesion during meiosis. *Nature.* 427:510–517. https://doi.org/10.1038/nature02312

Kitajima, T.S., T. Sakuno, K. Ishiguro, S. Iemura, T. Natsume, S.A. Kawashima, and Y. Watanabe. 2006. Shugoshin collaborates with protein phosphatase 2A to protect cohesin. *Nature.* 441:46–52. https://doi.org/10.1038/nature04663

Knop, M., F. Barr, C.G. Riedel, T. Heckel, and C. Reichel. 2002. Improved version of the red fluorescent protein (drFP583/DsRed/RFP). *Biotechniques.* 33:592–602: 594: 596–598 passim. https://doi.org/10.2144/02333rr02

Li, R., and A.W. Murray. 1991. Feedback control of mitosis in budding yeast. *Cell.* 66:519–531. https://doi.org/10.1016/0092-8674(81)90015-5

Li, Y., J. Bachant, A.A. Alcasabas, Y. Wang, J. Qin, and S.J. Elledge. 2002. The mitotic spindle is required for loading of the DASH complex onto the kinetochore. *Genes Dev.* 16:183–197. https://doi.org/10.1101/gad.959402

Liu, D., M. Vleugel, C.B. Backer, T. Hori, T. Fukagawa, I.M. Cheeseman, and M.A. Lampson. 2010. Regulated targeting of protein phosphatase 1 to the outer kinetochore by KNL1 opposes Aurora B kinase. *J. Cell Biol.* 188: 809–820. https://doi.org/10.1083/jcb.201001006

London, N., and S. Biggins. 2014. Signalling dynamics in the spindle checkpoint response. *Nat. Rev. Mol. Cell Biol.* 15:736–747. https://doi.org/10.1038/nrm3888

London, N., S. Ceto, J.A. Ranish, and S. Biggins. 2012. Phosphoregulation of Spc105 by Mps1 and PP1 regulates Bub1 localization to kinetochores. *Curr. Biol.* 22:900–906. https://doi.org/10.1016/j.cub.2012.03.052

Longtine, M.S., A. McKenzie III, D.J. Demarini, N.G. Shah, A. Wach, A. Brachat, P. Philippsen, and J.R. Pringle. 1998. Additional modules for versatile and economical PCR-based gene deletion and modification in Saccharomyces cerevisiae. *Yeast.* 14:953–961. https://doi.org/10.1002/(SICI)1097-0061(199807)14:10<953::AID-YEA293>3.0.CO;2-U

Marston, A.L. 2015. Shugoshins: tension-sensitive pericentromeric adaptors safeguarding chromosome segregation. *Mol. Cell. Biol.* 35:634–648. https://doi.org/10.1128/MCB.01176-14

Marston, A.L., and K. Wassmann. 2017. Multiple Duties for Spindle Assembly Checkpoint Kinases in Meiosis. *Front. Cell Dev. Biol.* 5:109. https://doi.org/10.3389/fcell.2017.00109

Marston, A.L., B.H. Lee, and A. Amon. 2003. The Cdc14 phosphatase and the FEAR network control meiotic spindle disassembly and chromosome segregation. *Dev. Cell.* 4:711–726. https://doi.org/10.1016/S1534-5807(03)00130-8

Marston, A.L., W.H. Tham, H. Shah, and A. Amon. 2004. A genome-wide screen identifies genes required for centromeric cohesion. *Science.* 303: 1367–1370. https://doi.org/10.1126/science.1094220

Meadows, J.C., L.A. Shepperd, V. Vanoosthuyse, T.C. Lancaster, A.M. Sochaj, G.J. Buttrick, K.G. Hardwick, and J.B. Millar. 2011. Spindle checkpoint silencing requires association of PP1 to both Spc7 and kinesin-8 motors. *Dev. Cell.* 20:739–750. https://doi.org/10.1016/j.devcel.2011.05.008

Meyer, R.E., S. Kim, D. Obeso, P.D. Straight, M. Winey, and D.S. Dawson. 2013. Mps1 and Ipl1/Aurora B act sequentially to correctly orient chromosomes on the meiotic spindle of budding yeast. *Science.* 339: 1071–1074. https://doi.org/10.1126/science.1232518

Monje-Casas, F., V.R. Prabhu, B.H. Lee, M. Boselli, and A. Amon. 2007. Kinetochore orientation during meiosis is controlled by Aurora B and the monopolin complex. *Cell.* 128:477–490. https://doi.org/10.1016/j.cell.2006.12.040

Neiman, A.M. 2011. Sporulation in the budding yeast Saccharomyces cerevisiae. *Genetics.* 189:737–765. https://doi.org/10.1534/genetics.111.127126

Newnham, L., P.W. Jordan, J.A. Carballo, S. Newcombe, and E. Hoffmann. 2013. Ipl1/Aurora kinase suppresses S-CDK-driven spindle formation during prophase I to ensure chromosome integrity during meiosis. *PLoS One.* 8:e83982. https://doi.org/10.1371/journal.pone.0083982

Niedzialkowska, E., F. Wang, P.J. Porebski, W. Minor, J.M. Higgins, and P.T. Stukenberg. 2012. Molecular basis for phosphospecific recognition of histone H3 tails by Survivin paralogues at inner centromeres. *Mol. Biol. Cell.* 23:1457–1466. https://doi.org/10.1091/mbc.e11-11-0904

Nijenhuis, W., G. Vallardi, A. Teixeira, G.J. Kops, and A.T. Saurin. 2014. Negative feedback at kinetochores underlies a responsive spindle

checkpoint signal. *Nat. Cell Biol.* 16:1257–1264. https://doi.org/10.1038/ncb3065

Peplowska, K., A.U. Wallek, and Z. Storchova. 2014. Sgo1 regulates both condensin and Ipl1/Aurora B to promote chromosome biorientation. *PLoS Genet.* 10:e1004411. https://doi.org/10.1371/journal.pgen.1004411

Pinsky, B.A., C.R. Nelson, and S. Biggins. 2009. Protein phosphatase 1 regulates exit from the spindle checkpoint in budding yeast. *Curr. Biol.* 19: 1182–1187. https://doi.org/10.1016/j.cub.2009.06.043

Primorac, I., J.R. Weir, E. Chiroli, F. Gross, I. Hoffmann, S. van Gerwen, A. Ciliberto, and A. Musacchio. 2013. Bub3 reads phosphorylated MELT repeats to promote spindle assembly checkpoint signaling. *eLife.* 2: e01030. https://doi.org/10.7554/eLife.01030

Rabitsch, K.P., J. Gregan, A. Schleiffer, J.P. Javerzat, F. Eisenhaber, and K. Nasmyth. 2004. Two fission yeast homologs of Drosophila Mei-S332 are required for chromosome segregation during meiosis I and II. *Curr. Biol.* 14:287–301. https://doi.org/10.1016/j.cub.2004.01.051

Robinett, C.C., A. Straight, G. Li, C. Willhelm, G. Sudlow, A. Murray, and A.S. Belmont. 1996. In vivo localization of DNA sequences and visualization of large-scale chromatin organization using lac operator/repressor recognition. *J. Cell Biol.* 135:1685–1700. https://doi.org/10.1083/jcb.135.6.1685

Rosenberg, J.S., F.R. Cross, and H. Funabiki. 2011. KNL1/Spc105 recruits PP1 to silence the spindle assembly checkpoint. *Curr. Biol.* 21:942–947. https://doi.org/10.1016/j.cub.2011.04.011

Salic, A., J.C. Waters, and T.J. Mitchison. 2004. Vertebrate shugoshin links sister centromere cohesion and kinetochore microtubule stability in mitosis. *Cell.* 118:567–578. https://doi.org/10.1016/j.cell.2004.08.016

Saurin, A.T. 2018. Kinase and Phosphatase Cross-Talk at the Kinetochore. *Front. Cell Dev. Biol.* 6:62. https://doi.org/10.3389/fcell.2018.00062

Scherthan, H., H. Wang, C. Adelfalk, E.J. White, C. Cowan, W.Z. Cande, and D.B. Kaback. 2007. Chromosome mobility during meiotic prophase in Saccharomyces cerevisiae. *Proc. Natl. Acad. Sci. USA.* 104:16934–16939. https://doi.org/10.1073/pnas.0704860104

Shepperd, L.A., J.C. Meadows, A.M. Sochaj, T.C. Lancaster, J. Zou, G.J. Buttrick, J. Rappsilber, K.G. Hardwick, and J.B. Millar. 2012. Phosphodependent recruitment of Bub1 and Bub3 to Spc7/KNL1 by Mph1 kinase maintains the spindle checkpoint. *Curr. Biol.* 22:891–899. https://doi.org/10.1016/j.cub.2012.03.051

Shirk, K., H. Jin, T.H. Giddings Jr., M. Winey, and H.G. Yu. 2011. The Aurora kinase Ipl1 is necessary for spindle pole body cohesion during budding yeast meiosis. *J. Cell Sci.* 124:2891–2896. https://doi.org/10.1242/jcs.086652

Shonn, M.A., R. McCarroll, and A.W. Murray. 2000. Requirement of the spindle checkpoint for proper chromosome segregation in budding yeast meiosis. *Science.* 289:300–303. https://doi.org/10.1126/science.289.5477.300

Shonn, M.A., A.L. Murray, and A.W. Murray. 2003. Spindle checkpoint component Mad2 contributes to biorientation of homologous chromosomes. *Curr. Biol.* 13:1979–1984. https://doi.org/10.1016/j.cub.2003.10.057

Straight, A.F., A.S. Belmont, C.C. Robinett, and A.W. Murray. 1996. GFP tagging of budding yeast chromosomes reveals that protein-protein interactions can mediate sister chromatid cohesion. *Curr. Biol.* 6: 1599–1608. https://doi.org/10.1016/S0960-9822(02)70783-5

Suzuki, A., A. Gupta, S.K. Long, R. Evans, B.L. Badger, E.D. Salmon, S. Biggins, and K. Bloom. 2018. A Kinesin-5, Cin8, Recruits Protein Phosphatase 1 to Kinetochores and Regulates Chromosome Segregation. *Curr. Biol.* 28: 2697–2704.e3. https://doi.org/10.1016/j.cub.2018.08.038

Sym, M., J.A. Engebrecht, and G.S. Roeder. 1993. ZIP1 is a synaptonemal complex protein required for meiotic chromosome synapsis. *Cell.* 72: 365–378. https://doi.org/10.1016/0092-8674(93)90114-6

Tanaka, T.U., N. Rachidi, C. Janke, G. Pereira, M. Galova, E. Schiebel, M.J. Stark, and K. Nasmyth. 2002. Evidence that the Ipl1-Sli15 (Aurora kinase-INCENP) complex promotes chromosome bi-orientation by altering kinetochore-spindle pole connections. *Cell.* 108:317–329. https://doi.org/10.1016/S0092-8674(02)00633-5

Tien, J.F., N.T. Umbreit, D.R. Gestaut, A.D. Franck, J. Cooper, L. Wordeman, T. Gonen, C.L. Asbury, and T.N. Davis. 2010. Cooperation of the Dam1 and Ndc80 kinetochore complexes enhances microtubule coupling and is regulated by aurora B. *J. Cell Biol.* 189:713–723. https://doi.org/10.1083/jcb.200910142

Tsuchiya, D., C. Gonzalez, and S. Lacefield. 2011. The spindle checkpoint protein Mad2 regulates APC/C activity during prometaphase and metaphase of meiosis I in Saccharomyces cerevisiae. *Mol. Biol. Cell.* 22: 2848–2861. https://doi.org/10.1091/mbc.e11-04-0378

Tsuchiya, D., Y. Yang, and S. Lacefield. 2014. Positive feedback of NDT80 expression ensures irreversible meiotic commitment in budding yeast. *PLoS Genet.* 10:e1004398. https://doi.org/10.1371/journal.pgen.1004398

Verzijlbergen, K.F., O.O. Nerusheva, D. Kelly, A. Kerr, D. Clift, F. de Lima Alves, J. Rappsilber, and A.L. Marston. 2014. Shugoshin biases chromosomes for biorientation through condensin recruitment to the pericentromere. *eLife.* 3:e01374. https://doi.org/10.7554/eLife.01374

Wang, F., J. Dai, J.R. Daum, E. Niedzialkowska, B. Banerjee, P.T. Stukenberg, G.J. Gorbsky, and J.M. Higgins. 2010. Histone H3 Thr-3 phosphorylation by Haspin positions Aurora B at centromeres in mitosis. *Science.* 330: 231–235. https://doi.org/10.1126/science.1189435

Warren, C.D., D.M. Brady, R.C. Johnston, J.S. Hanna, K.G. Hardwick, and F.A. Spencer. 2002. Distinct chromosome segregation roles for spindle checkpoint proteins. *Mol. Biol. Cell.* 13:3029–3041. https://doi.org/10.1091/mbc.e02-04-0203

Yamagishi, Y., T. Honda, Y. Tanno, and Y. Watanabe. 2010. Two histone marks establish the inner centromere and chromosome bi-orientation. *Science.* 330:239–243. https://doi.org/10.1126/science.1194498

Yamagishi, Y., C.H. Yang, Y. Tanno, and Y. Watanabe. 2012. MPS1/Mph1 phosphorylates the kinetochore protein KNL1/Spc7 to recruit SAC components. *Nat. Cell Biol.* 14:746–752. https://doi.org/10.1038/ncb2515

Yang, Y., D. Tsuchiya, and S. Lacefield. 2015. Bub3 promotes Cdc20-dependent activation of the APC/C in S. cerevisiae. *J. Cell Biol.* 209: 519–527. https://doi.org/10.1083/jcb.201412036

Yoon, H.J., and J. Carbon. 1999. Participation of Bir1p, a member of the inhibitor of apoptosis family, in yeast chromosome segregation events. *Proc. Natl. Acad. Sci. USA.* 96:13208–13213. https://doi.org/10.1073/pnas.96.23.13208

Yu, H.G., and D. Koshland. 2007. The Aurora kinase Ipl1 maintains the centromeric localization of PP2A to protect cohesin during meiosis. *J. Cell Biol.* 176:911–918. https://doi.org/10.1083/jcb.200609153

Supplemental material

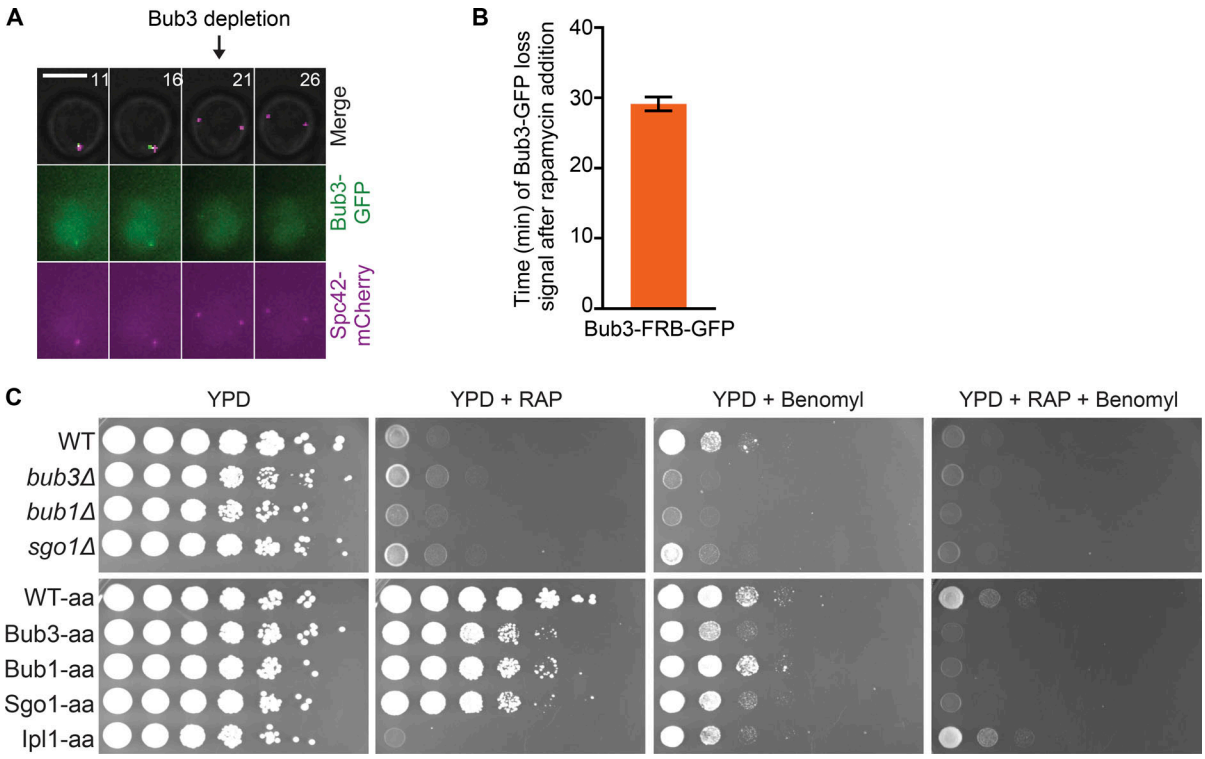

Figure S1. **Bub3 is depleted from the nucleus upon rapamycin addition. (A)** Representative time lapse of Bub3-FRB-GFP cell wherein rapamycin is added at t = 0 min to visualize when Bub3 is anchored away from the nucleus (when GFP focus was no longer visible). Bub3-FRB is tagged with GFP and Spc42 is tagged with mCherry. Scale bars, 5 µm. **(B)** Graph of the mean time of Bub3 nuclear depletion after rapamycin addition. 100 cells from two independent experiments were monitored. Error bars represent SEM. **(C)** Mitotic growth of different strains with and without rapamycin and benomyl addition. Cultures are serially diluted 1:10 from a saturated yeast culture. Rapamycin does not affect the mitotic growth of the anchor-away strains due to their genetic background (*tor1-1* mutation). However, the strains without the *tor1-1* mutation are sensitive to rapamycin (wild-type, *bub3Δ*, *bub1Δ*, and *sgo1Δ*). Final concentrations of benomyl and rapamycin were 15 µg/ml and 1 µg/ml, respectively. The plates were incubated at 30°C for 36–40 h before imaging. aa, anchor away.

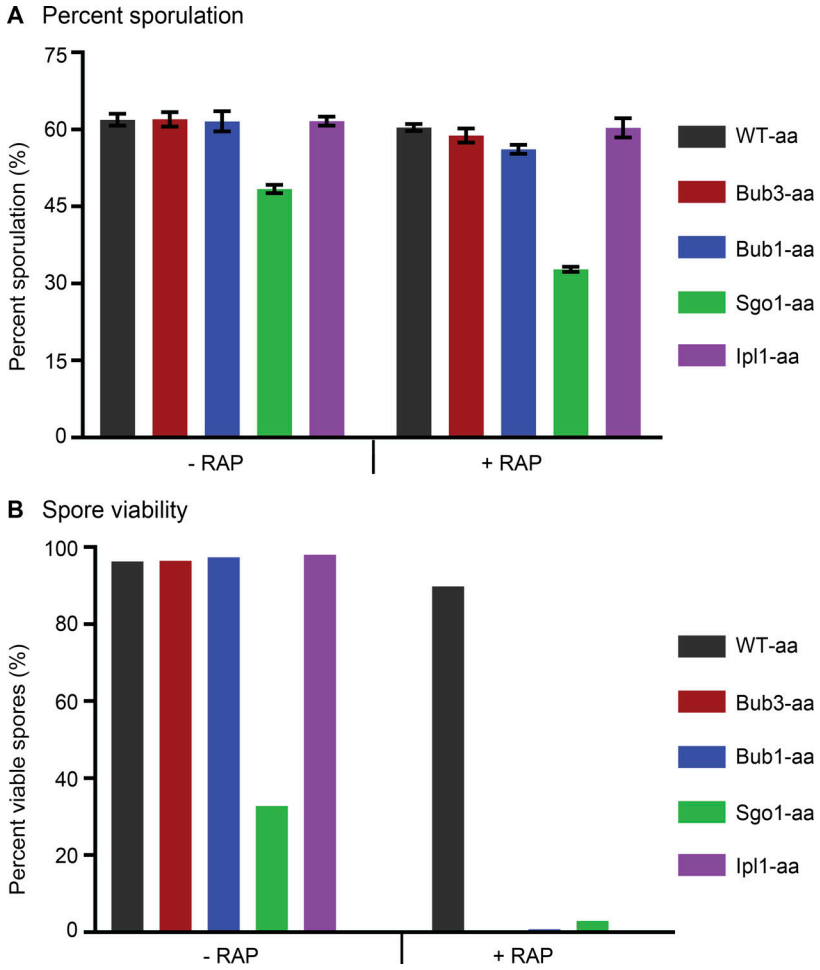

Figure S2. **Anchor away of Bub3, Bub1, Sgo1, and Ipl1 upon rapamycin addition causes loss of spore viability. (A)** Percent sporulation of Bub3-aa, Bub1-aa, Sgo1-aa, and Ipl1-aa cells with or without rapamycin. Data obtained from three independent experiments. Error bars represent SEM. **(B)** Spore viability of wild-type and Bub3-aa, Bub1-aa, Sgo1-aa, and Ipl1-aa cells with and without rapamycin. Data were obtained by analyzing the growth of ≥240 spores for each genotype. aa, anchor away.

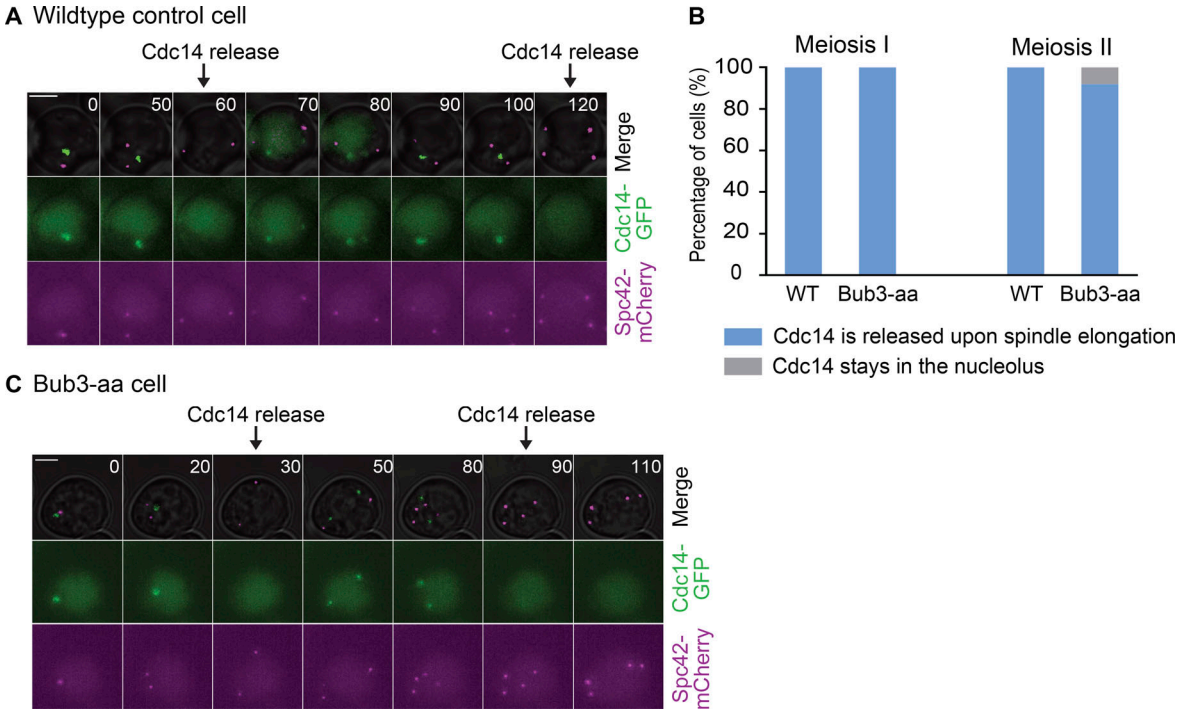

Figure S3. **Premature spindle elongation in cells with nuclear depletion of Bub3 coincides with Cdc14-GFP nucleolar release. (A)** Representative time-lapse images of a wild-type anchor-away control cell. Cell expresses Cdc14-GFP and Spc42-mCherry. Time 0 represents prophase I. Scale bar, 5 µm. **(B)** Percentage of wild-type cells and cells with nuclear depletion of Bub3 wherein Cdc14 was either released or kept in the nucleolus upon spindle elongation. **(C)** Representative time-lapse images of a cell with nuclear depletion of Bub3. Cell expresses Cdc14-GFP and Spc42-mCherry. Time 0 represents prophase I. Scale bar, 5 µm.

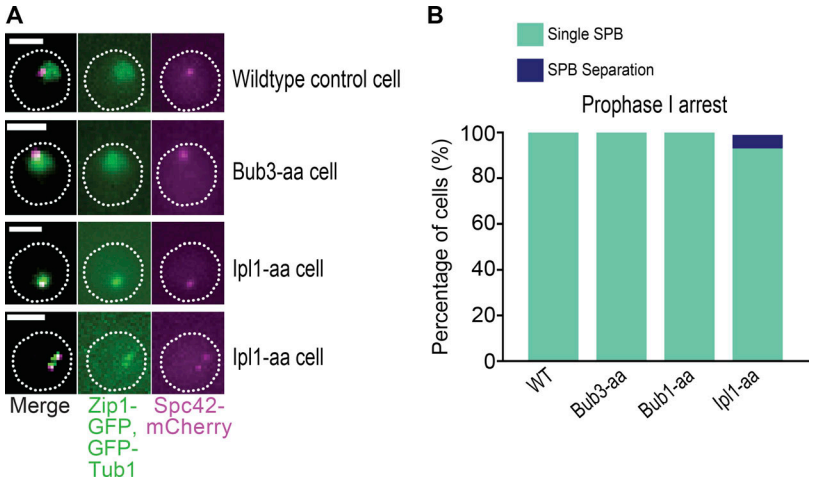

Figure S4. **Cells with nuclear depletion of Bub3, Bub1, or Ipl1 rarely form spindles in prophase I. (A)** Representative images of a wild-type anchor-away control cell and cells with Bub3 or Ipl1 anchored away with rapamycin addition. The cells have a deletion of *NDT80* so that they do not exit prophase I. Cell expresses Zip1-GFP, Tub1-GFP, and Spc42-mCherry. Scale bars, 5 µm. **(B)** Percentage of wild-type cells and cells with nuclear depletion of Bub3, Bub1, or Ipl1 with a single SPB or premature SPB separation. aa, anchor away.

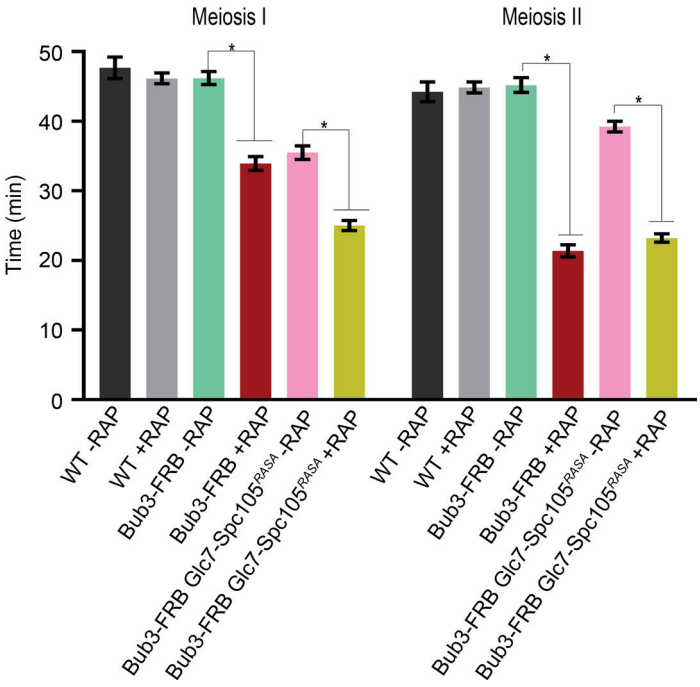

Figure S5. **Glc7 tethered to SPC105^{RASA} results in a somewhat faster meiosis I and II.** Graph of wild-type cells, cells with nuclear depletion of Bub3, and cells with nuclear depletion of Bub3 but expressing Spc105^{RASA} fused with Glc7 under the *SPC105* promoter and at the endogenous location. Rapamycin is added 7 h after resuspension in sporulation medium. Error bars represent SEM. At least 100 cells from two or more independent experiments per genotype were monitored. Asterisks indicate a statistically significant difference compared with wild-type cells (*, P < 0.05, Mann-Whitney test).

Table S1 is provided online as a separate Excel file and lists the *S. cerevisiae* strains used in this study.